Environment, Development and Sustainability
https://doi.org/10.1007/s10668-026-07530-y

Verticalization and microclimatic dynamics: Impacts on environmental conditions in open public spaces of a Tropical Coastal City, João Pessoa, Brazil

Guilhardo Barros Moreira de Carvalho[1] · Luiz Bueno da Silva[1] · Ricardo Victor Rodrigues Barbosa[2] · Erivaldo Lopes de Souza[1]

Received: 3 May 2024 / Accepted: 7 March 2026

Abstract
This study analyzes the association between urban morphology, microclimate, and thermal comfort in tropical urban areas, focusing on João Pessoa, a city characterized by a hot and humid climate. The research aims to investigate how different urban configurations, considering varying degrees of verticalization and vegetation coverage, influence thermal conditions and thermal comfort in the built environment. Using computational simulation methods with the ENVI-MET software and thermal indices (PET and UTCI), the study examines three urban modification scenarios to assess the impact of population growth through vertical expansion on urban environmental quality. Climatic data obtained from meteorological stations and local measurements were used to perform computational simulations, enabling model validation with real-world data. The results indicate that verticalization significantly reduces the sky view factor (SVF), negatively affecting ventilation and increasing urban temperatures. Green spaces, however, proved effective in mitigating urban heat island effects, enhancing thermal comfort. The findings have direct implications for sustainable urban planning, emphasizing the importance of integrating green strategies, utilizing more efficient surface materials, and managing building density to improve thermal quality and public space comfort. These aspects are particularly relevant for urban policies in tropical cities, fostering more effective adaptation to climate change.

Keywords Urban morphology · Thermal comfort · Envi-met

✉ Guilhardo Barros Moreira de Carvalho
guilhardo.carvalho@academico.ufpb.br

[1] Federal University of Paraíba, João Pessoa, Brazil

[2] Federal University of Alagoas, Maceió, Brazil

Published online: 09 April 2026

1 Introduction

Urban growth and construction irregularities nequire effective urban planning to address socio-environmental issues. Various research on urban environmental quality informs public policies by analyzing urban dynamics and the natural environment for sustainability. Investigating the direct relationship between urban occupation, topography, and climate is crucial for developing effective urban planning strategies. Scientific literature supports the correlation between urban microclimates and land utilization factors (Chan & Chau, 2021; Fachinello Krebs & Johansson, 2021; Feng et al., 2024; Fiorillo et al., 2023; Kotharkar & Dongarsane, 2024; Hashemi et al., 2023; Wu et al., 2019).

Urban morphology, including land use planning, significantly influences the environmental quality shaped by climate (Apreda et al., 2023; Battisti et al., 2018; Bedra et al., 2023; Li et al., 2023; Wu et al., 2018; Yi et al., 2022; Zhang et al., 2023a, 2023b; Zhao et al., 2023). Environmental quality debates consider density, built areas, and land use, impacting urbanization and comfort. Sustainable planning factors include roughness, porosity, density, orientation, and green areas.

Considering microclimates, built density, permeability, and material properties that affect temperature significantly shape identity and environmental quality. Vegetation plays a pivotal role in regulating microclimates, alongside reflective materials (Binabid & Anteet, 2024; da Silva, 2023; Ge et al., 2024; Kowe et al., 2024; Piercy et al., 2024; Stark da Silva et al., 2023; Susca et al., 2023; Xie et al., 2024; Yilmaz et al., 2020). Bioclimatic urbanism integrates environmental considerations for sustainable living.

Urban heat islands, stemming from land use and material properties, impact thermal comfort in public spaces (Acero et al., 2021; Altunkasa & Uslu, 2020; Feng et al., 2024; Fiorillo et al., 2023; Kotharkar & Dongarsane, 2024; Gusson & Duarte, 2016; Ramyar et al., 2019). Microclimatic studies prioritize adaptations aligning with urban diversity, emphasizing the importance of public spaces.

The impacts of urbanization on microclimate are more perceptible on clear-sky days with calm air, potentially resulting in heat islands (Aboelata & Sodoudi, 2019; Ascione et al., 2024; Bakhtyari et al., 2024; Boccalatte et al., 2023; Habibi & Kahe, 2024; Zhang et al., 2023a, 2023b). Public spaces, especially green ones, boost air quality and promote physical activity (Asfour et al., 2023; Binabid & Anteet, 2024; Boeri et al., 2023; Chatzinikolaou et al., 2018; Li et al., 2022; Yang et al., 2020). Furthermore, they strengthen the population's sense of belonging and identity, contributing to more sustainable and healthier cities.

Thermal comfort, a crucial aspect of the quality of life in built spaces, is assessed using indices such as PET (Physiologically Equivalent Temperature) and UTCI (Universal Thermal Climate Index) (da Silva, 2023; Lai et al., 2019, 2020; McRae et al., 2020a; Ribeiro et al., 2021; Roshan et al., 2019; Santamouris et al., 2018; Santana et al., 2023; Wai et al., 2022; Wu et al., 2018). Computational tools like ENVI-met and Rayman Pro analyze environmental performance across various scales (Brahimi et al., 2023; Feng et al., 2024; Kotharkar & Dongarsane, 2024; Lin & Gui, 2024; Liu et al., 2023; Sinsel et al., 2021). Research focuses on assessing the impact of high-rises on climatic variables and thermal comfort, utilizing computer simulation to explore different scenarios.

Despite the growing recognition of the effects of verticalization on the urban climate, the importance of public open spaces, and the role of urban green infrastructure in enhancing thermal comfort and sustainability in cities, a significant gap remains in understand-

ing how these interventions impact thermal quality across different urban configurations in hot and humid climates, particularly when analyzed through computational simulation. In particular, low-latitude hot-humid cities, such as those in northeastern Brazil, face unique challenges due to their specific climatic conditions and the lack of detailed studies on the effective application of green infrastructure in this context. (Aram et al., 2019; Blanco and Convertino, 2023; de Quadros and Mizgier, 2023)**.**

The theoretical foundation of this study is enriched by the incorporation and discussion of references in various urban, climatic, and geographic contexts. Dissanayake and Weerasinghe (2021), through a bibliometric mapping, emphasize the relevance of urban microclimate and outdoor thermal comfort in hot and humid cities, highlighting the necessity for integrated policies that consider local climatic specificities. Akhavan et al. (2025) address Industry 5.0 and its impacts on civil construction, discussing the role of technological innovations and systemic approaches in redesigning urban spaces and promoting thermal comfort. Conversely, de Souza e Silva et al. (2022) analyzed thermal comfort conditions in the Brazilian context, emphasizing the importance of urban vegetation in mitigating urban heat islands, especially in Northeastern cities—a reality directly comparable to João Pessoa.

The consistent discussion of these references in the introduction and literature review strengthens the study's rationale, justifying the methodological choices and the adopted geographic focus. Contextual statements such as Dissanayake and Weerasinghe (2021) highlighting the importance of integrating vegetation interventions into urban planning in cities subjected to high temperatures and humidity, and de Souza e Silva et al. (2022), when studying João Pessoa, emphasizing that urban vegetation is decisive for local thermal comfort, are recommended to reinforce the article's scientific positioning regarding originality, timeliness, and potential contribution to the academic literature in the area.

Furthermore, the literature review can be expanded by including advanced and recent works, such as those by Feng et al. (2024) and Yilmaz et al. (2021), which present evidence on the effectiveness of vegetation and innovative urban design in different international contexts. These studies deepen the debate on adaptable solutions for Brazilian cities, highlighting the use of simulations to optimize green area arrangements and evaluate the impact of materials and urban configurations on the microclimate. Thus, the article can offer more grounded and assertive recommendations for sustainable urban planning, evidencing the relevance of its findings in both local and global contexts.

The study starts from the central hypothesis that urban morphology, especially with varying levels of verticalization and vegetation cover, directly influences microclimatic conditions and thermal comfort in hot and humid cities like João Pessoa. The clear definition of hypotheses is essential to guide applied research in the field of climatic urbanism. This hypothesis was tested through simulations and measurements, whose results confirm that increased verticalization reduces the sky view factor (SVF), compromising ventilation and raising temperatures, while green areas work to mitigate urban heat effects and improve environmental comfort for public space users, evaluated through thermal indices such as PET and UTCI.

The article explicitly states that urban interventions, particularly those incorporating vegetation, can mitigate the negative impacts arising from high building density, thus validating the hypotheses raised. Studies such as Fernandes et al. (2020) and Leal and Barbosa (2022) support this evidence, indicating that increased building density is associated with higher

surface temperatures, greater heat retention, and reduced nighttime cooling, whereas vegetated areas promote positive effects on ventilation and thermal comfort.

The confirmation of these hypotheses provides robust support for formulating more effective public policies, especially in tropical cities exposed to increasing thermal extremes. Understanding these dynamics is relevant because tropical cities face specific challenges related to rising temperatures, public health, and urban quality of life, exacerbated by climate change. Research analyzing microclimates and thermal comfort offers scientific backing for sustainable urban adaptation policies, underpinning planning decisions, material selection, and the need to invest in green infrastructure, as observed in studies conducted in various cities across differing urban, climatic, and geographic contexts.

The relevance of the topic manifests not only in the face of the global climate emergency but also through the direct impacts on public health, urban quality of life, and social dynamics in public spaces. The literature highlights that tropical climate cities, such as João Pessoa, face particular challenges, among which urban heat islands, restricted ventilation, and thermal discomfort stand out—factors that significantly influence usage patterns, permanence, and citizen satisfaction in open areas. Recent scientific production in this field has expanded the repertoire of evidence on effective urban heat mitigation strategies, contributing to the design of healthier, adaptable, and resilient urban environments. Systematic reviews and advanced studies, such as Ferrarezi (2023) and Feng et al. (2024), reinforce the importance of integrated approaches that combine planning, technology, and ecology to promote thermal comfort and environmental sustainability.

Understanding research on urban microclimate and verticalization is imperative in tropical cities such as João Pessoa, where population growth (15.3% from 2010–2022) exacerbates urban heat islands, adversely affecting public health, utilization of open spaces, and energy efficiency. Such studies underpin sustainable urban planning policies, mitigating risks from climate change-intensified heatwaves while promoting socio-spatial equity in low-income areas.

In conclusion, the research seeks to aid sustainable urban planning by assessing local regulations, climatic variables, and their impact on thermal comfort in various conditions. Specifically focusing on ENVI-met's applicability in tropical cities, it provides insights into tackling challenges in Brazil's northeastern region.

To provide a comprehensive investigation, this article is structured as follows: Sect. 2 describes the study area, the applied scope, and its climatic and urban characteristics. Section 3 outlines the methodology, including data collection and processing (3.1.1), scenario definition and modeling (3.1.2), statistical analysis (3.2), and the simulation process (3.3). Section 3.3 discusses and analyzes the results, presenting the reliability test (4.1), sky view factor (4.2), air temperature (4.3), air humidity (4.4), wind speed (4.5), mean radiant temperature (4.6), and thermal comfort indices (4.7). Finally, Sect. 4.7 presents the conclusions, highlighting the main findings and their implications for urban climate studies and sustainable urban planning.

2 Study area

João Pessoa, the capital of Paraíba state in northeastern Brazil, boasts diverse neighborhoods, with the main banking district situated in the southern part of the city (Fig. 1). Positioned around latitude 7°08′44.0″ S, longitude 34°50′18.5″ W, and at an altitude of 43 m, the

city operates in the UTC-3 time zone. This residential area features a robust infrastructure, encompassing schools, hospitals, and recreational areas, catering to a population of varied socioeconomic backgrounds.

The population growth of 15.3% between 2010 and 2022 makes João Pessoa the capital of the Brazilian Northeast with the highest population increase during this period. Additionally, when compared to all cities in Brazil, the city recorded the fourth-largest growth, standing out as one of the urban centers that expanded the most in the country during this time (IBGE, 2023). This significant population increase may have important implications for urban planning and development, infrastructure, public services, and environmental impacts, making the study relevant for understanding urban growth dynamics in Brazil and seeking sustainable solutions for the challenges arising from this growth. As a tropical city, João Pessoa may be subject to the phenomenon of "urban heat islands" (Medeiros et al., 2023; Noda et al., 2022; Souza et al., 2016), and studying this phenomenon can help better understand the impacts of urbanization and develop strategies for reducing urban heat. The research aims to deepen the understanding of the relationship between verticalization, greenery, public open spaces, and urban environments, exploring verticalization and urban heat, with an emphasis on the use of computational simulations in hot and humid low-latitude climates.

In a microclimatic study, delineating the study area within the Bancários neighborhood (Fig. 2) is essential for computer simulations. This approach provides detailed information about the local microclimate, identifying specific climate patterns, aiding in understanding climate phenomena, assessing thermal comfort, and planning interventions. The study focuses on a residential section known as “3 Ruas.”.

For configuring climate data and analyzing simulated results in computational studies, a city's climate description is essential. Derived from a 30-year historical dataset, the INMET Normais Climatológicas offers a comprehensive understanding of the region's climatic conditions. From 1991 to 2020, João Pessoa experiences its highest temperatures from October

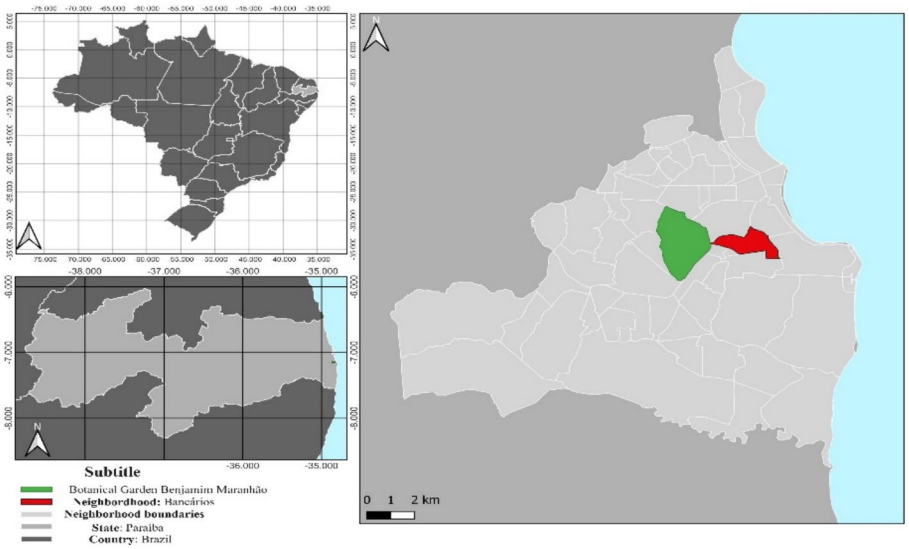

Fig. 1 Location of the study.Source: Authors (2025)

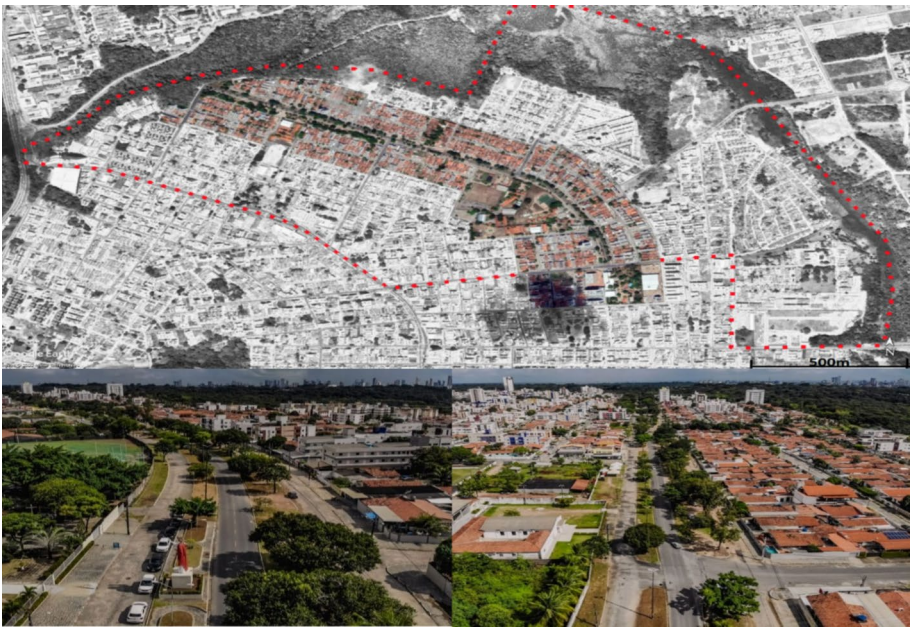

Fig. 2 The defined territory (in colors) and photographs.Source: Author (2025), compiled from TF5, João Pessoa Hall portals

to May, with prevailing winds from the east and southeast. The city has a rainy season between April and July, followed by drier months from October to December. Average monthly temperatures range from 24 °C to 28 °C, peaking in February and lowest between June and August. (INMET, 2022).

The research focuses on a specific sector comprising three residential streets, designated for building development with varying heights owing to the prevalence of single-family residential lots. The increased density is driven by the proximity of two universities and historical population growth. This sector, located within a corridor connecting the city center, coastal area, and outlying neighborhoods, acts as a catalyst for urban expansion.

The definition of this area is justified by its land use and occupation, significant tree presence along the main road axis, and inclination towards high-rise structures. The analysis involves the current occupancy model and building surveys and aims to create hypothetical scenarios for simulations. The objective is to enhance the understanding of microclimate and offer insights for sustainable urban planning.

3 Methodology

To analyze the urban microclimate and its relationship with building performance in different urban scenarios, a mixed-methods approach was applied. This methodology was chosen due to its ability to integrate quantitative and qualitative data, enabling a comprehensive assessment of microclimatic interactions. The study aims to evaluate the hypothesis that urban form and building typology influence microclimatic conditions and thermal comfort

in a hot and humid tropical climate. Furthermore, it seeks to examine whether urban interventions, such as increasing building heights and incorporating vegetation cover and open spaces, can mitigate the effects of urban heat.

The methodological approach follows five stages. Stage 1 established the theoretical foundation through a literature review on urban microclimate modeling, thermal comfort indices, and the role of urban morphology in modifying local climatic conditions. This stage ensured that the research aligned with existing knowledge while identifying gaps that this study aims to address.

Stage 2 utilized data from the National Institute of Meteorology (INMET) and cartographic sources to conduct scenario modeling. In Stage 4, urban microclimate simulations were performed using ENVI-MET, generating data and maps. Specifically, microclimatic variables and thermal comfort indices (PET and UTCI) were collected every 30 min on 11/23/2019 using Rayman Pro software.

Stage 3 – During this stage, on-site surveys were conducted to assess land use and occupation characteristics, measure climatic variables, acquire climatic data, and gather cadastral and cartographic information about the study area. The construction materials adopted in the simulation were defined based on the field survey, identifying the most used materials in buildings within the study area. Following the data collection and survey phase, the scenario design and modeling were carried out for the simulation process.

In Step 5, the attention turned to analyzing the results, specifically the correlation between the Sky View Factor (SVF) and microclimatic variables (air temperature, relative air humidity, air speed, and mean radiant temperature) at a height of 1.5 m in different scenarios. Statistical calculations (means, standard deviation, RMSE, and Spearman correlation coefficients) were conducted by statistical guidelines (Blaine, 2023) using RStudio. Validating the accuracy of simulated data enhances the overall understanding of identifiable spatial patterns.

Key studies that informed this research include Oke et al. (2017), Bruse and Fleer (1998), Matzarakis et al. (2007, 2010), and recent applications in tropical urban climates (Aboelata and Sodoudi, 2019; Erlwein & Pauleit, 2021; Norouziasas et al., 2022; Gamero-Salinas et al., 2022; Yi et al., 2023).

3.1 Data and methodolody

3.1.1 Data collection and processing

As detailed in Step 2, Simulations were conducted for both current and hypothetical scenarios using climate data reflecting elevated temperatures and reduced humidity, characteristic of the hot-dry season chosen to simulate potential temperature rises in the city due to climate change, based on the 1991–2020 Climatological Normal. November, representing the hot-dry period, was specifically selected for this study (INMET, 2022).

The study encompasses both primary and secondary data sources to develop simulation scenarios. The primary data includes on-site climate measurements conducted. A portable mini-station was utilized for the field data collection on November 9, 2022, from 8 am to 5 p.m., utilizing the HOBO U10–003 Temp/RH/2 external channels from Onset. The device recorded temperature and relative humidity at 30-min intervals. The climatic data were obtained from INMET stations (A320) and (82,798), encompassing air temperature,

relative humidity, specific air humidity at 2,500 m high, wind speed and direction, solar radiation, cloudiness, soil humidity, and other variables.

Specific air humidity data were sourced from the digital library of the Department of Atmospheric Sciences at the University of Wyoming, referencing the Natal Airport station due to its proximity to João Pessoa. The remaining data were extracted from records of the INMET automatic station in João Pessoa, covering the period from 2000 to 2022. November 23, 2019, was identified as the day with the highest maximum temperature for conducting the simulation, Table 1.

In-situ measurements of climate variables (air temperature and humidity) were conducted to validate the simulated conditions (Gusson, 2020; Gusson & Duarte, 2016; Shinzato et al., 2019; Silva et al., 2020). Data was collected at climatological stations in the city, including the automatic station (A320) and the conventional station (82,798). The analysis point, located in “Três Ruas" (latitude 7°8′40" S and longitude 34°50′35" W), close to a municipal school, was selected for its east/west orientation, ensuring continuous direct solar radiation throughout the day. The definition of statistical methods followed the guidelines of Blaine (2023), ensuring the consistency and reliability of the data.

3.1.2 Scenario definition and modeling

In Stage 2, the study models three urban transformation scenarios. Building modeling involves two cases: replacing single-family homes and single-story commercial buildings and adding multifamily and/or commercial structures. Existing vertical buildings remain, applying lot remembrance techniques for those undergoing high-rise, following urban legislation setbacks and heights. Vertical models consider three levels: low, medium, and high-rise, reflecting the neighborhood context.

These configurations describe the trends in urbanization and urban legislation in the city, based on the year of this study. The division of the study area into Zones A, B, and C allows for a spatial analysis of the impacts of urban form on microclimatic conditions and the patterns and limitations of the computational simulation.

The study area, divided into sectors A, B, and C, includes scenarios 1, 2, and 3, as shown in Fig. 3. In Scenario 1, 192 lots with the potential for renovation maintain their template for specific functions, while 650 lots are identified for renovation, encompassing residences and businesses up to one floor. Scenario 2 comprises medium high-rise (up to 10 floors), with 203 lots designated for 10-story buildings. Scenario 3 involves a high-rise (up to 20 floors), with 197 lots designated for 20-story buildings.

The subsequent stage involves creating and modification of the simulation file, specifying the geographic location and grid size, and inserting bitmap files to delineate zones. Corrections to the geographic north ensure spatial accuracy, with details added about terrain, soil, buildings, vegetation, and receptors. Scenarios incorporate standardized construction materials consistent with the current city standard.

Lots are waterproofed with concrete, roads utilize materials like asphalt and cobblestone, and sidewalks are constructed with gray concrete or earth. Buildings consist of burnt ceramic bricks, often with white paint or coating, and roofs adhere to the pattern of ceramic and metallic tiles, aiming to blend with the existing environment and maintain consistency with the city's prevalent style.

Table 1 Representative day during the hot–dry period (UTC-3).Source: INMET (2022)

Measurement date	Measurement Time (UTC)	Hourly Total Precipitation (mm)	Atmospheric Pressure at Station Level, Hourly (mb)	Atmospheric Pressure Reduced to Sea Level (mB)	Global Radiation (Kj/m^2)	Air temperature – Dry Bulb, Hourly (ºC)	Dew point temperature (ºC)	Maximum temperature in the previous hour (ºC)	Minimum temperature in the previous hour (ºC)	Maximum relative humidity in the previous hour (%)	Minimum relative humidity in the previous hour (%)	Relative humidity, hourly (%)	Wind, hourly, wind Direction (degrees)	Wind Maximim fust (m/s)	Wind, hourly. Wind speed (m/s)
23/11/2019	0	0	1008,8	1015,1	−3,5	26,3	20,9	26,3	26,1	72	70	72	122	6,6	1,2
	300	0	1007,4	1013,7	−3,5	25,7	20,7	25,9	25,7	74	72	74	130	4	0,6
	600	0	1006,6	1012,91	−3,5	25	20,5	25,2	24,8	77	75	76	127	3,1	0,6
	900	0	1007,8	1014,09	173,6	26,3	20,8	26,3	24,8	77	72	72	101	3,2	1,1
	1200	0	1009,1	1015,35	1936,2	28,6	19,1	30	28,3	60	54	57	108	5	1,6
	1500	0	1007,4	1013,6	3202,8	30,7	19,3	31,5	29,6	54	49	51	106	5,1	1,3
	1800	0	1006,2	1012,42	2075,2	29,3	20,4	30,6	29,1	59	54	59	104	6,5	1,5
	2100	0	1007	1013,28	7,3	26,4	20,1	27,1	26,4	69	65	68	98	6	1,6
	2300	0	1008	1014,29	−3,5	26,2	20,3	26,3	26,1	71	70	70	98	4,6	1

Fig. 3 Location and division.Source: Authors (2025)

3D modeling divides the area into sectors and segments for data analysis, including various environmental factors. Simulations assess microclimatic performance and thermal comfort across the scenarios. Construction materials adhere to the city standard.

3.2 Statistical analysis

Statistical tests were conducted to validate the hypothesis that variations in urban form have a significant effect on microclimatic conditions. The correlations between Sky View Factor (SVF) and microclimatic variables (air temperature, relative humidity, wind speed, and mean radiant temperature) at 1.5 m above ground level were assessed using Spearman's correlation coefficients. The choice of Spearman's method was justified by its robustness in analyzing nonlinear relationships in environmental datasets (Blaine, 2023).

Statistical measures, such as mean, standard deviation, and Root Mean Square Error (RMSE), were also included to compare observed and simulated data. The RMSE and R^2 metrics were employed to validate the accuracy of ENVI-met simulations against field measurements. Statistical analyses and graph development were performed in RStudio using the R programming language.

The methodological approach is structured based on selected urban climate studies, a reliability assessment, comparing simulated results with on-site data for air temperature and humidity, is conducted using metrics such as RMSE and R^2 (Aboelata and Sodoudi,

2019; Erlwein and Pauleit, 2021; Habibi and Kahe, 2024; Jamei et al., 2023; Norouziasas et al., 2022; Sayad et al., 2024). These steps constitute a comprehensive process from setup to result in analysis, contributing to a thorough understanding of the simulated conditions.

3.3 The simulation process

The simulation process, as outlined in step 4, follows a systematic, multistep approach (Bruse & Fleer, 1998; McRae et al., 2020a, 2020b; Shinzato et al., 2019; Sinsel et al., 2022). The first step defines a $180 \times 180 \times 35$ cell grid with parameters such as $2 \times 2 \times 3$ m per cell and a 2% telescopic method in the vertical grid. Deleting information in border cells streamlines the process. The climatic and geographical data of the study area were added.

The subsequent stage involves creating and modification of the simulation file, specifying the geographic location and grid size, and inserting bitmap files to delineate zones. Corrections to the geographic north ensure spatial accuracy, with details added about terrain, soil, buildings, vegetation, and receptors. Scenarios incorporate standardized construction materials consistent with the current city standard.

Lots are waterproofed with concrete, roads utilize materials like asphalt and cobblestone, and sidewalks are constructed with gray concrete or earth. Buildings consist of burnt ceramic bricks, often with white paint or coating, and roofs adhere to the pattern of ceramic and metallic tiles, aiming to blend with the existing environment and maintain consistency with the city's prevalent style.

In each simulation, the starting time of 9 p.m. from previous simulations on November 21, 2019, is used. The initial 27 simulated hours are omitted for necessary software adjustments, focusing the analysis on the 24 h of November 23, 2019. Results, extracted as data and maps, are converted into Excel spreadsheets, and graphical representations are created using the Leonardo 3.1 plug-in. The analysis prioritizes central areas for reliability, overlooking instabilities at the map edges.

Thermal comfort analysis in João Pessoa on November 23, 2019, employed Rayman Pro 3.1 Beta software (Matzarakis et al., 2007, 2010). PET and UTCI indices were calculated, considering air temperature, mean radiant temperature relative humidity, wind speed, and personal data, with specific conditions configured in the software.

Additionally, personal data outlined by ISO 8996/2004 were considered, including height (1.75 m), weight (70 kg), age (35), and sex (male). The activity level was set at 165 W/m^2 (295 W), equivalent to light walking activity on a flat surface at 4 km/h. Thermal insulation of clothing was defined as 0.5 Clo, indicating summer attire per ISO 7730/2005. Data analysis was conducted at 6 am/pm, 9 am/pm, 12 pm, and 3 pm, following recommendations from the WMO. All times were adjusted to the local study time to better align with the UTC-3 application. Reliability testing employed metrics such as RMSE and R^2.

To calculate the SVF, SketchUp's Sky View Analysis plugin was employed, based on Oke et al. (2017) theory (Gamero-Salinas et al., 2022; Yi et al., 2023), providing detailed data about the SVF from the 3D.

The model calibration process was carried out to ensure the reliability of the results obtained for the Sky View Factor (SVF) and the thermal indices PET (Physiologically Equivalent Temperature) and UTCI (Universal Thermal Climate Index) Table 2. Calibration involved comparing simulated data from the ENVI-met software with field measurements and reference data from the INMET A320 meteorological station, aiming to minimize

discrepancies and adjust specific model parameters according to local characteristics. Key parameters adjusted included the roughness coefficient, adapted to represent the influence of buildings on air circulation, as well as the initial wind speed and soil moisture distribution, refined based on local measurements to better represent relative humidity and interaction with the urban microclimate.

Model validation and calibration followed internationally established benchmarks, including calculating the Root Mean Square Error (RMSE), which showed an average difference of 0.81 °C for air temperature and 2.13% for relative humidity, values consistent with recent studies (Feng et al., 2022; Habibi & Kahe, 2024; Sayad et al., 2024; Zheng et al., 2023). Additionally, the Pearson correlation coefficient (R) was 0.85 between measured and simulated data, indicating a strong correlation and high model adherence to reality. For analyzing the relationship between SVF, temperature, and humidity, the Spearman correlation coefficient (r) was used, supporting the validity of the observed patterns consistent with other methodological reference studies.

This calibration process, aligned with best practices for using ENVI-met in urban microclimate simulations, enhanced the robustness and reliability of the results, allowing the model to accurately reflect local thermal conditions. This is fundamental for supporting policies and urban interventions aimed at mitigating heat islands and promoting thermal comfort in tropical urban environments. However, it is recommended to continue calibration in future studies to address specific scenarios and configurations to broaden the applicability of the simulated climate models.

The incorporation of validation with multiple sources strengthens the reliability of the results obtained through computational simulation, certifying its applicability for the analysis and study of urban climate adaptation strategies and mitigation of heat and climate change.

Table 2 Calibration parameters and referencesSource: Authors (2025)

Parameter	Adjusted Value/Reference	References
RMSE Temperature (°C)	0.81	Feng et al. (2022), et al
RMSE Relative Humidity (%)	2.13	Habibi and Kahe (2024)
Pearson R (temperature & humidity)	0.85	Sayad et al. (2024), et al
Roughness/Conductivity	Locally calibrated	Local literature and Oke (1988)
PET Indices	Calibration conducted in similar urban and climatic context	Andrade et al. (2016), Souza and Katzschner (2018), Leal and Barbosa (2022)

Therefore, by providing an extensive methodological framework, this section promotes clarity in data handling, scenario delineation, and analytical procedures, contributing to the credibility and application of the study in urban climate research.

4 Results and speeches

4.1 Reliability test

The study examined temperature and relative humidity disparities between measured, simulated, and INMET station (A320) values on November 9, 2022, from 8 am to 5 p.m. Both measured and simulated scenarios were analyzed to explore variations influenced by urbanized surroundings. Environmental differences were observed between the measured and simulated locations compared to the less urbanized A320 station. Temperature divergences between the simulation and station A320 ranged from 0.23 °C to 1.82 °C, with the largest difference at 1 pm and the smallest at 5 pm, consistent with the station's less urbanized setting.

Measured data variations ranged from −2.58 °C to −0.27 °C, with the greatest difference recorded at 8:00 and the smallest at 17:00. The percentage discrepancies between simulated values and the A320 station ranged from −9% to 2%, with the largest difference at 8:00 and the smallest at 17:00. Compared to measured data, percentage variations were 1% to 8%, with the smallest difference at 16:00 and the largest at 10:00 and 11:00.

Statistical tests (RMSE and R^2) revealed a very strong correlation of 0.85 between measured and simulated data, indicating the model's adequate representation of variables. Differences of 0.81ºC and 2.13% for air temperature and humidity, respectively, suggest an acceptable representation of the model for both variables, as illustrated in Fig. 4.

Although there are small discrepancies, the trends of the variables simulated by the model are deemed appropriate. However, they indicate margins of error that may affect more detailed analyses. For instance, the temperature variation from −2.58 °C to −0.27 °C suggests that, in certain periods, local conditions might not be accurately represented by the model, likely due to limitations in spatial resolution or the configuration of climatic factors.

Similarly, percentage differences in humidity, although below 3%, may influence the accuracy of simulations dependent on this variable, such as thermal comfort indices. Nevertheless, the overall reliability of the model is reinforced by the low RMSE values, combined with the strong correlation of 0.85 between measured and simulated data, which strengthens

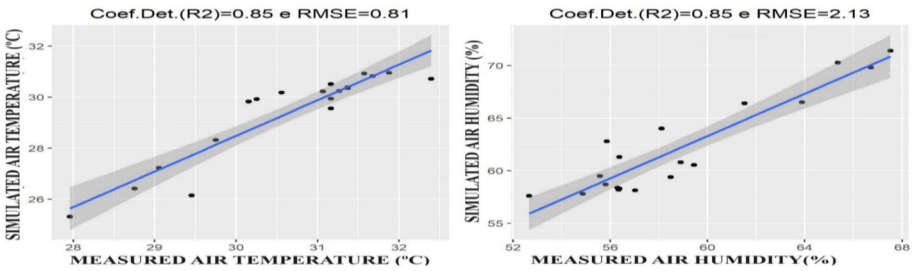

Fig. 4 Correlation between measured and simulated data.Source: Authors (2025)

its applicability for medium-term or urban-scale analyses. The reported RMSE and R^2 values indicate the model's reliability and, being within the range observed in previous studies (Feng et al., 2022; Habibi and Kahe, 2024; Sayad et al., 2024; Zheng et al., 2023), support its adjustment and alignment with the literature. Caution is advised when extrapolating the results to highly localized microclimatic analyses, taking into account the need for further adjustments and calibrations for specific scenarios.

4.2 Sky view factor (SVF)

Sectors A, B, and C display SVF variations in scenarios 1A, 2A, 3A, 1B, 2B, 3B, 1C, 2C, and 3C, respectively, indicating the impact of verticalization on microclimate and thermal comfort. The results underscore that increased verticalization consistently reduces SVF across all sectors. Notable changes occur in Sector B, with R1 and R2 experiencing significant SVF decreases of 0.59 and 0.56, respectively. In Sector C, R2 records a maximum SVF decrease of 0.52. In Sector A, R1 exhibits a slight SVF decrease of 0.06 due to tree presence, while R3 shows a modest decrease of 0.08 on the north side. R5 in Sector A also experienced a 0.06 SVF decrease, positioned near a construction site with trees and a 15-story building.

In Sector C, R1 experiences a modest decrease of 0.02 SVF due to verticalization, while R5 observes a modest decrease of 0.08 SVF attributed to immediate surroundings with residential buildings up to three floors. Table 3 offers comprehensive SVF values for all receivers, highlighting nuanced variations influenced by specific characteristics like tree coverage or vacant land. These subtleties are essential for understanding the effects of verticalization on microclimate and thermal comfort.

4.3 Air temperature

Data analysis indicates consistent thermal patterns in receptors across sectors throughout the day, as shown in Fig. 5. Across all sectors, temperatures rise after dawn, peak in the afternoon, and decline in the evening due to solar influence. In Sector A, temperatures range from 24.5 to 31 °C across all receptors, with scenario 3A showing slightly lower temperatures, particularly in the early morning and late evening. Sector B displays similar thermal behavior, with temperatures ranging from 25 to 30.5 °C. In Sector C, temperatures range from approximately 24.5 to 30.5 °C across receptors. Temperature averages across different time bands reveal consistent patterns, with the highest averages observed in the afternoon, indicating significant warming possibly due to direct solar radiation. Lower temperatures are recorded during the night and early morning hours.

Table 3 SVF values.Source: Authors (2025)

RECEIVER	SCENARIOS								
	SECTOR A			**SECTOR B**			**SECTOR C**		
	1A	2A	3A	1B	2B	3A	1C	2C	3C
R1	0,64	0,64	0,58	0,88	0,47	0,29	0,7	0,7	0,68
R2	0,73	0,5	0,43	0,87	0,47	0,31	0,84	0,5	0,32
R3	0,79	0,78	0,71	0,7	0,5	0,4	0,8	0,71	0,62
R4	0,78	0,64	0,49	0,79	0,57	0,42	0,81	0,69	0,57
R5	0,54	0,53	0,48	0,87	0,58	0,38	0,67	0,64	0,59
R6	0,84	0,57	0,46	0,77	0,59	0,37	0,76	0,65	0,58

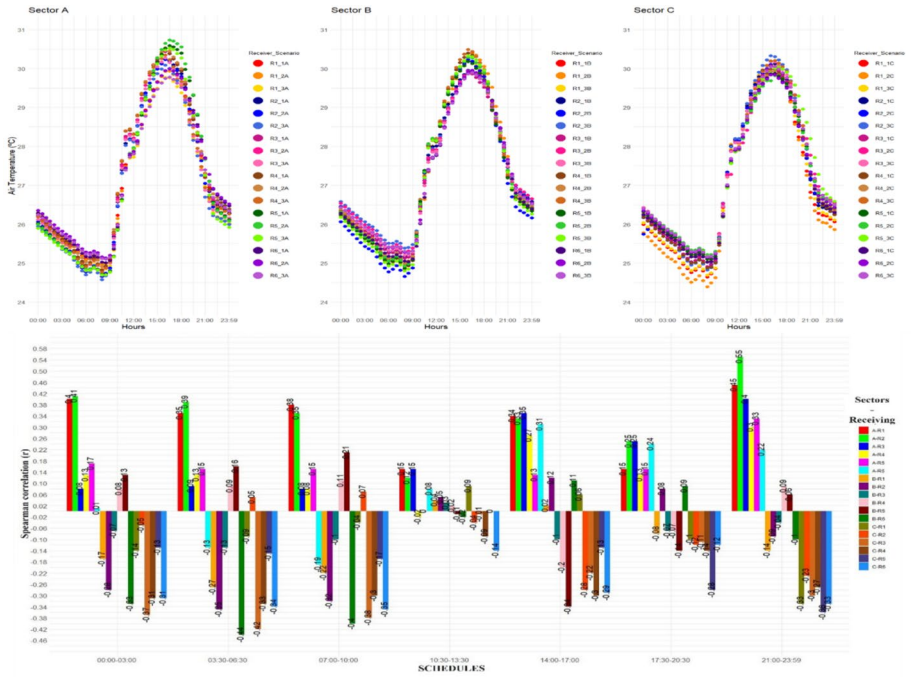

Fig. 5 Air temperature behavior and spearman correlation coefficient- SCC (r) of SVF and air temperature.Source: Authors (2025)

Statistical analysis, using Spearman's Correlation Coefficient (r), revealed predominantly weak and non-statistically significant correlations ($p > 0.05$) between SVF and air temperature in the three sectors. A moderate correlation stands out in Sector A for receiver R2 at 21:00–23:59 and 00:00–03:00. It was observed that in the time bands 00:00–03:00, 14:00–17:00, 17:30–20:30 and 21:00–23:59, there is a positive correlation between SVF and the temperature of the air, indicating a joint increase. In the ranges of 03:30–06:30, 07:00–10:00, and 10:30–13:30, there is a negative correlation, suggesting an increase in temperature with a decrease in SVF. Figure 5 shows the correlations between SVF and air temperature in all evaluated receivers.

Most correlations are weak in sectors B and C, without statistical significance. These correlations vary between receptors and time bands, with the influence of factors such as solar exposure and materials. In summary, the results highlighted that correlations between SVF and air temperature vary in strength and significance over different periods, portraying the complex interaction between solar exposure, urban configuration, and surface material properties.

The highest temperature averages in Sector A (above 29.64 °C) between 14:00–17:00 indicated significant warming, likely due to direct solar radiation. Similarly, Sector B presented higher averages (above 29.65 °C) between 14:00–17:00, with lower averages (between 25.31 °C and 26.27 °C) during the night and early morning. In Sector C, the highest averages (above 29.66 °C) were recorded between 14:00–17:00, while the lowest averages occurred during the night and early morning (between 25.31 °C and 26 °C).

The temperature variation between time slots for each receiver highlights that different receivers show different patterns of variation over the 24 h, providing insights into the specific behavior of each receiver about temperature changes during the day. About the temperature variation between the time bands for each receiver, it is highlighted that R5 presented the largest variation of 5.25 °C, while R6 had the smallest variation, with 4.33 °C over the 24 h. The other receptors varied between 4.39 °C (R1), 4.9 °C (R2), 4.97 °C (R3) and 4.99 °C (R4). Greater standard deviations were observed in time bands with more intense thermal variations, such as 17:30–20:30, suggesting the influence of solar insolation and thermal exchanges in these periods. Time bands with lower insolation, such as 00:00–03:00 and 03:30–06:30, have smaller standard deviations, indicating greater consistency in temperatures between scenarios during these bands.

The data analysis shows that urban geometry, shading, and the thermal properties of building materials directly influence temperature variations throughout the day. The Sky View Factor (SVF), related to solar exposure and shading, exhibits weak correlations with air temperature, indicating that these variables indirectly affect temperature. During the night, a negative correlation between SVF and temperature suggests that more shaded areas have lower temperatures due to reduced solar exposure. However, in the afternoon, when solar radiation is more intense, the positive correlation between SVF and temperature indicates that increased solar exposure raises the temperature.

We can also observe the significant role of thermal properties of materials, with concrete and asphalt having high thermal capacity, absorbing heat during the day and releasing it at night, contributing to greater temperature variations. The largest temperature variations were found in areas more exposed to the sun or with less shading, while more protected areas or those with thermal insulation materials showed more consistent temperatures. Urban geometry, including verticalization and building configuration, affects the heat exchange between the environment and buildings, with greater thermal deviation during periods of higher solar insolation. Areas with more solar exposure or little thermal protection showed more pronounced temperature fluctuations, while areas with greater shading or building protection exhibited more stable temperatures.

Examined at different times within the sectors, different patterns emerge throughout the day, highlighting the influence of solar exposure, verticalization, and urban configuration on spatial temperature variations. The detailed analysis reveals consistent thermal trends, emphasizing the impact of solar radiation and variations across urban sectors. These findings underscore the importance of incorporating considerations responsive to climatic conditions and solar orientation in architectural design, promoting adaptive and energy-efficient solutions.

4.4 Air humidity

Figure 6 illustrates diurnal humidity variations across sectors, with receptors ranked by airspeed: R3, R6, R1, R4, R5, and R2. In sector A, humidity in R2 fluctuates from 74.56% during 03:30–06:30 to lower averages of 52.7–54.55% during 14:00–17:00. Time intervals 10:30–13:30, 14:00–17:00, and 17:30–20:30 exhibit the lowest averages due to solar influence. Weak correlations between SVF and humidity predominate, with occasional exceptions.

Sector B experiences peak humidity during 03:30–06:30 and minimum levels during 14:00–17:00. Similar to sector A, intervals 10:30–13:30, 14:00–17:00, and 17:30–20:30 show the lowest averages influenced by solar exposure. The SVF-humidity correlation in sector B demonstrates variable patterns. In sector C, humidity peaks during 03:30–06:30 and reaches its lowest during 14:00–17:00. Time intervals of 10:30–13:30, 14:00–17:00, and 17:30–20:30 register the lowest averages due to solar influence. Weak correlations between SVF and humidity are evident.

The Spearman's Correlation Coefficient (r) was applied, based on Blaine's (2023) guidelines, to analyze the correlation between the FVC and air humidity, Fig. 6 shows the correlations between SVF and air humidity in all evaluated receivers. In Sector A, weak and moderate correlations were observed, with correlation coefficients (r) ranging from $-0.40 < r < 0.40$. Certain time intervals showed an inverse relationship between FVC and air humidity, with p-values below 0.05, indicating that a decrease in FVC may correspond to an increase in humidity. Notable receptors include R1 (00:00–03:00; $r = -0.48$) and R2 (00:00–03:00; $r = -0.50$), both with p-values below 0.05.

In Sector B, diverse patterns were found, with some intervals showing negative correlations and others positive. For example, receptors R2 (00:00–03:00; $r = 0.70$), R6 (00:00–03:00; $r = 0.74$), R2 (03:30–06:30; $r = 0.72$), and R6 (03:30–06:30; $r = 0.79$) displayed strong

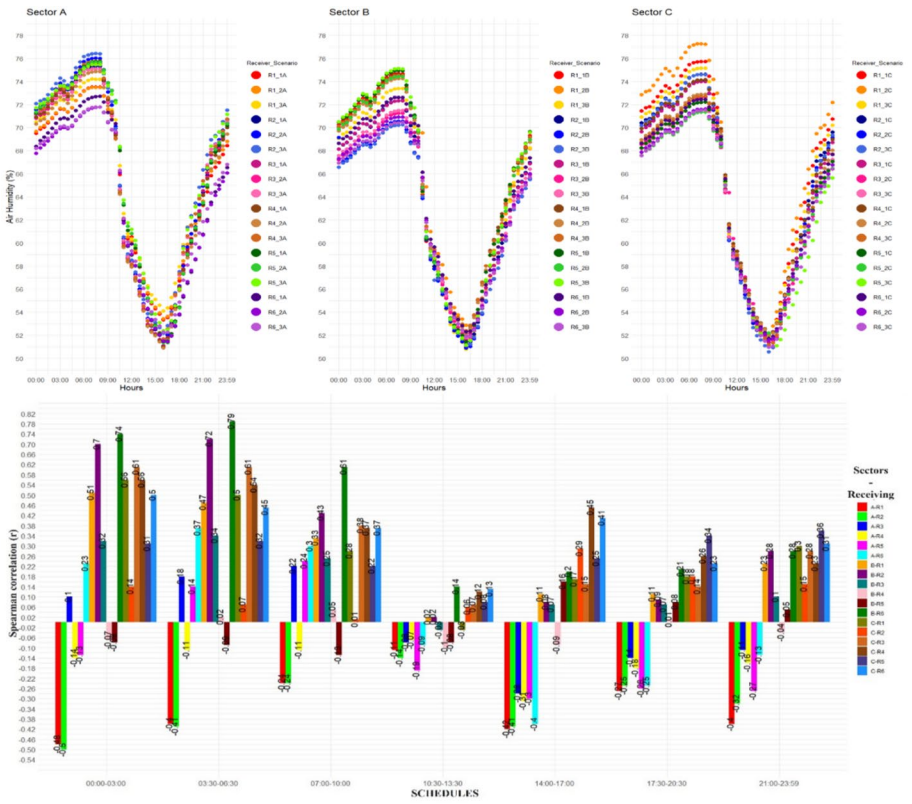

Fig. 6 Air humidity behavior SCC (r) of SVF and Air humidity.Source: Authors (2025)

correlations, while R1 (00:00–03:00; r = 0.51) and R2 (07:00–10:00; r = 0.43) showed moderate correlations, all with p-values below 0.05. In Sector C, correlations ranged from weak to moderate, with p-values below 0.05. Strong correlations, such as R3 (00:00–03:00; r = 0.61) and R3 (03:30–06:30; r = 0.61), indicated a stronger relationship, while moderate correlations included R1 (00:00–03:00; r = 0.56), R4 (00:00–03:00; r = 0.56), and R6 (00:00–03:00; r = 0.50). The results suggest that the relationships between FVC and air humidity are complex and depend on various factors, highlighting the need for further optimization in the analysis to better understand urban dynamics.

The data analysis indicates that the effects of shading, the thermal properties of building materials, and urban geometry play significant roles in shaping the diurnal humidity variations across sectors. The Sky View Factor (SVF), which influences solar exposure and shading, shows weak to moderate correlations with humidity levels in all sectors, suggesting that while shading may influence humidity, the relationship is complex and not entirely direct. Humidity levels varied throughout the day, with peaks during the night (03:30–06:30) and drops in the afternoon (14:00–17:00), when solar radiation is most intense. This behavior suggests that shading can reduce direct solar exposure and, consequently, decrease evaporation, resulting in higher humidity. Areas with lower Sky View Factor (SVF) values, meaning more shaded areas, tend to show higher humidity during the cooler hours of the night, while areas with higher SVF values, more exposed to the sun, show lower humidity levels during the day due to intensified evaporation from solar heating.

The correlation between SVF and humidity varies in a complex manner across different periods. In the early morning hours, areas with greater shading or less solar exposure tend to maintain higher humidity levels due to reduced evaporation. In more sun-exposed areas with higher SVF, there are more significant reductions in humidity during periods of higher solar radiation, due to increased evaporation. It was observed that the influence of shading is also evident, as areas with less solar exposure retain more humidity during cooler periods, while those more exposed to the sun exhibit lower humidity due to higher evaporation from solar radiation. This behavior between solar exposure, shading, and airflow contributed to humidity variations, with the relationship between SVF and humidity reflecting the complex dynamics between these environmental variables.

The thermal properties of building materials also affect humidity behavior. Materials such as concrete and asphalt have high thermal mass, absorbing heat during the day and releasing it at night. This heat retention performance certainly reduces the cooling effect in shaded areas, resulting in more consistent humidity levels. In contrast, areas with materials of lower thermal mass or more exposed to solar radiation showed faster cooling and more fluctuating humidity, especially in the afternoon. Urban geometry, including building verticality and the density of the urban design, also influenced airflow and shading. Areas with tall buildings create more shaded environments, which tend to maintain higher humidity levels at night. However, during the day, these areas experience lower humidity due to reduced airflow and greater thermal mass absorption.

Spatial analysis unveils distinct humidity patterns across sectors, shaped by solar exposure, shading, and ventilation. Overall, consistent diurnal variations in average humidity, along with SVF-humidity correlations, indicate the impacts of environmental factors on humidity dynamics.

4.5 Airspeed

Figure 7 shows airspeed averages across sectors. In sector A, airspeed ranged from 0.3 to 0.85 m/s, with an average of 0.55 m/s. In 1A, R1 and R2 led, followed by 2A and 3A, with differences up to 0.15 m/s. Sector B's R1 had the highest speed in 2B, followed by 1B and 3B. In sector C, R1 exhibited a decrease and stabilization, with 3C recording higher speeds.

Standard deviations of airspeed between scenarios revealed diverse patterns in all sectors, indicating varied influences on air circulation. Correlation analysis (p-value < 0.05) between Sky View Factor (SVF) and airspeed revealed significant correlations in all sectors. The sector-specific analysis highlighted a notable reduction in ventilation with increased verticalization, particulary in scenarios 3B in Sector B and 3C in Sector C.

The Spearman's Correlation Coefficient (r) was applied, based on Baline's (2023) guidelines, to analyze the correlation between the FVC and air humidity. In Sector A, weak and moderate correlations were observed, with correlation coefficients (r) ranging from $-0.40 < r < 0.40$. Certain time intervals showed an inverse relationship between FVC and air humidity, with p-values below 0.05, indicating that a decrease in FVC may correspond to an increase in humidity.

Notable receptors include R1 (00:00–03:00; $r = -0.48$) and R2 (00:00–03:00; $r = -0.50$), both with p-values below 0.05. In Sector B, diverse patterns were found, with some intervals showing negative correlations and others positive. For example, receptors R2 (00:00–03:00;

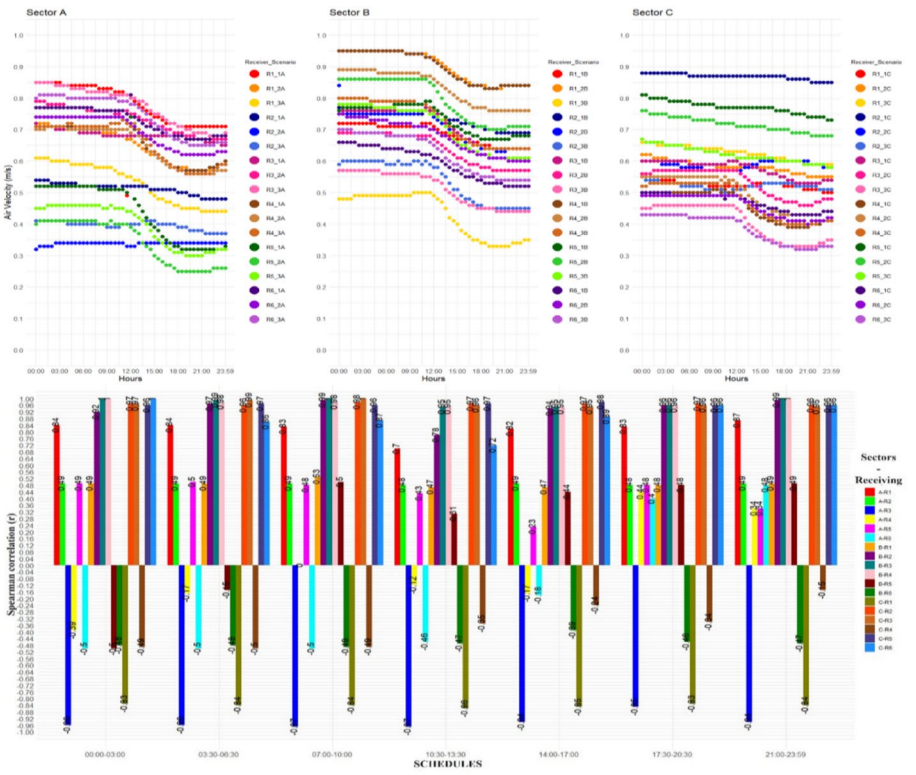

Fig. 7 Airspeed behavior and SCC (r) of SVF and airspeed.Source: Authors (2025)

r=0.70), R6 (00:00–03:00; r=0.74), R2 (03:30–06:30; r=0.72), and R6 (03:30–06:30; r=0.79) displayed strong correlations, while R1 (00:00–03:00; r=0.51) and R2 (07:00–10:00; r=0.43) showed moderate correlations, all with p-values below 0.05.

In Sector C, correlations ranged from weak to moderate, with p-values below 0.05. Strong correlations, such as R3 (00:00–03:00; r=0.61) and R3 (03:30–06:30; r=0.61), indicated a stronger relationship, while moderate correlations included R1 (00:00–03:00; r=0.56), R4 (00:00–03:00; r=0.56), and R6 (00:00–03:00; r=0.50). The results suggest that the relationships between FVC and air humidity are complex and depend on various factors, highlighting the need for further optimization in the analysis to better understand urban dynamics.

The analysis of the obtained data reveals a significant influence of shading effects, construction material properties, and urban geometry on thermal variations across different sectors. It was observed that the correlations between the Sky View Factor (SVF) and airspeed, as well as between SVF and humidity, highlight the substantial impact of shading on thermal comfort regulation and ventilation. Areas with lower SVF, meaning those with more shading, exhibited reduced ventilation and higher humidity levels. In scenarios with increased building verticalization and decreased SVF, ventilation circulation was lower, leading to greater humidity retention. This association demonstrates the influence of shading in reducing evaporation, which consequently increases humidity in the environment.

Urban geometry, particularly verticalization, plays a crucial role in thermal dynamics and ventilation. The data showed that increased verticalization reduced airspeed, creating areas with poor air circulation and consequently higher temperatures. In highly verticalized sectors, the negative correlation between SVF and airspeed indicates that the high density of buildings acts as a barrier to airflow, forming stagnation zones with greater heat and humidity accumulation.

The analysis in the sectors reveals the general trend of expansion, throughout the day, of the least efficient air circulation areas, highlighting the preponderant role of verticalization in modulating air speeds. Negative correlations imply that reduced SVF correlates with increased airspeed, possibly due to buildings acting as barriers. Conversely, positive correlations suggest that reduced SVF corresponds to decreased airspeed, influenced by urban porosity and roughness. The results reinforce the importance of considering the built environment in urban ventilation. Identifying affected areas highlights the need to strategically plan the density and layout of buildings, balancing verticalization and open spaces, and establishing a basis for urban interventions aimed at thermal comfort and environmental quality.

4.6 Mean radiant temperature

Figure 8 illustrates mean radiant temperature (MRT) averages in three sectors. Sector A shows thermal variations ranging from 15 °C to 71 °C, with a notable increase post-17:00. Sector B displays uniform behavior, with a range from 14 °C to 72 °C, and a noticeable rise after 5:00 pm. In sector C, temperatures range from 15 °C to 74 °C, with similar patterns during specific time intervals. Analysis reveals cyclical trends in MRT, likely influenced by environmental factors.

The highest MRT averages, exceeding 54.98 °C, occur between 2 and 5 pm due to low humidity, high temperatures, and low air speeds. Intermediate averages of 22.45 °C to 24.85 °C are observed from 9 pm to 11:59 p.m. Similar temperature variations occur in sectors B and C, with significant differences in receptors R3 and R5.

The correlation between Sky View Factor (SVF) and MRT in the sectors revealed interesting associations, highlighting positive and negative relationships between SVF and MRT, suggesting influences from urban porosity and wind tunnels. When analyzing the MRT maps at specific times in scenarios A, B, and C, significant variations were observed throughout the day, highlighting the influence of urban geometry, surface materials, and the presence of vegetation.

In sector A, we noticed significant correlations between SVF and MRT in different receivers, with R1 showing strong correlations in different time bands (00:00–03:00/03:30–06:30/07:00–10:00; $0.62 < r < 0.68$; $p\_value < 0.05$). Comprehensive analyses revealed interesting associations between SVF and MRT, highlighting positive (R2, R5, R6) and negative (R1, R3, R4) relationships, suggesting influences from urban porosity and wind tunnels.

The correlations in sector B, especially with R1, R2, and R3, indicated a direct relationship between greater permeability, SVF and lower solar exposure, with lower MRT. In sector C, correlations ranged from moderate to very strong, reinforcing the connection between permeability, solar exposure, and thermal variations during the day.

Correlations between SVF and MRT show intriguing associations, indicating both positive and negative relationships. In sector A, R1 displays strong correlations, emphasizing varied relationships between SVF and MRT. In sector B, correlations with R1, R2, and R3

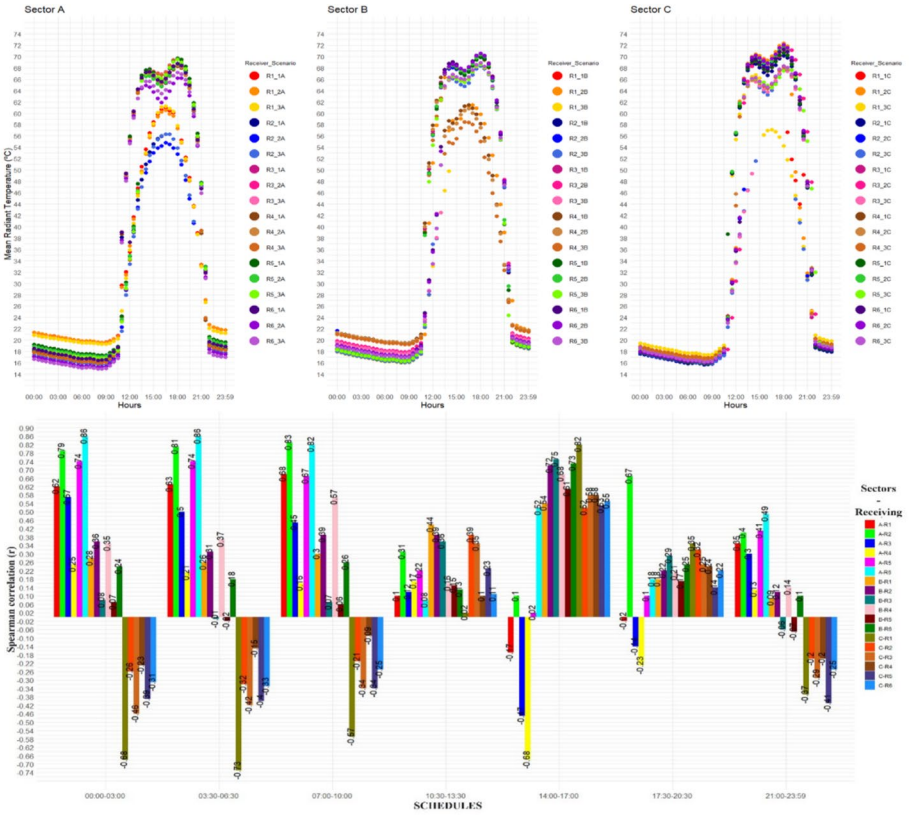

Fig. 8 MRT behavior and SCC (r) of the SVF and MRT.Source: Authors (2025)

suggest a direct relationship between greater permeability (SVF) and reduced solar exposure, resulting in lower MRT. In sector C, correlations reinforce the connection between permeability, solar exposure, and thermal variations during the day. These findings underscore the significance of urban factors in influencing MRT and thermal comfort.

The data indicates the significant influence of shading effects, heat retention properties of construction materials, and urban geometry on variations in Mean Radiant Temperature (MRT) observed across the studied sectors. The positive and negative associations in the correlations between Sky View Factor (SVF) and MRT suggest that heat diffusion and solar radiation exposure are influenced by urban porosity and building configuration.

MRT fluctuations exhibited cyclical patterns, with maximum values exceeding 54.98 °C between 2:00 PM and 5:00 PM, when relative humidity was low, air temperatures were high, and wind speeds were reduced. Urban geometry, particularly building verticalization and its configuration, plays a critical role in MRT behavior. Strong correlations between SVF and MRT highlight the impact of urban openness and wind corridors on thermal dispersion. The correlations indicate that higher SVF values are associated with lower solar exposure, resulting in lower MRT values.

Construction materials also exert a significant effect, as surfaces with high heat retention capacity contributed to elevated MRT levels during the day and delayed thermal dissipation at night. These findings reinforce the importance of selecting materials with low thermal inertia and high reflectance as key strategies for mitigating urban heat.

Analyzed climatic variables are crucial for understanding thermal comfort in urban environments, impacting people's comfort perception. Yet a comprehensive assessment requires integrating indices like PET and UTCI. Connecting climatic variables with thermal comfort indices is vital for quantifying their impact on thermal sensations. This alignment is essential for effective urban planning, building design, and climate adaptation strategies. Nonetheless, discrepancies in mean radiant temperature between 13:00 and 20:00 underline the need for improved simulation accuracy through robust calibration approaches. The analysis of climatic variables and the application of thermal comfort indices are crucial for sustainable solutions in architecture and urbanism.

4.7 Thermal comfort indexes

The PET and UTCI thermal comfort indices, depicted in Fig. 9, illustrate various scenarios and times in Sectors A, B, and C in João Pessoa on November 23, 2019. The PET index values were calibrated based on previous studies conducted in Salvador, with a climate akin to João Pessoa. This calibration was applied in João Pessoa and Maceió, both situated on the Brazilian northeastern coast (Andrade and Romero, 2018; de Souza & Katzschner, 2018; Leal & Barbosa, 2022). These studies categorized the PET index into four levels: “very hot” (PET ≥ 34.1ºC), “hot” (34.1ºC > PET > 29.4ºC), “not very hot” (29.4ºC > PET > 26.8ºC), and “comfortable” (PET ≤ 26.8ºC).

Receivers R1, R2, and R3 in scenarios 1A, 2A, and 3A showed varying indices throughout the day. For example, in scenario 1A, R1 at 06:00 had a PET of 20.5ºC and a UTCI of 24.7ºC, reaching 43.7ºC and 37.5ºC at 15:00, then returning to 28.7ºC (PET) and 29.8ºC (UTCI) at 21:00. R2 in scenario 1 showed reasonable comfort at 06:00 (PET 19.8ºC, UTCI 24.1ºC) and moderate discomfort at 15:00 (PET 42.6ºC, UTCI 36.9ºC). Receptors R4, R5,

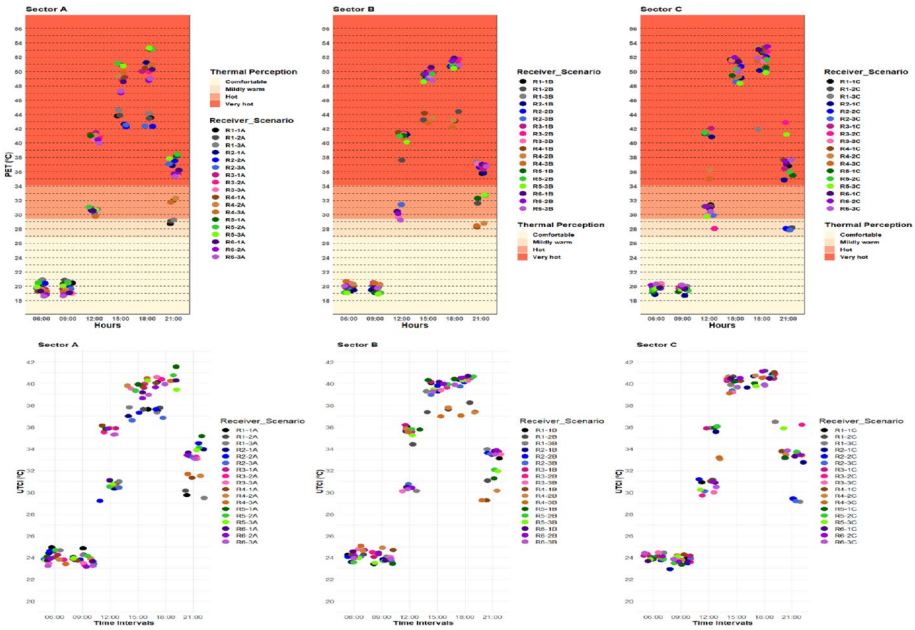

Fig. 9 PET and UTCI.Source: Authors (2025)

and R6 exhibited similar patterns, with indices peaking during the hottest hours (15:00), indicating thermal discomfort.

In Scenario B, sector B's receivers maintained relatively stable thermal indices, ranging from 19.1ºC to 50.7ºC (PET) and 23.7ºC to 40.5ºC (UTCI) throughout the day. Variances leading to thermal discomfort were observed in Scenarios 1 C, 2 C, and 3C. For instance, in Scenario 1 C, receptor R1 displayed a PET of 19.3ºC and UTCI of 23.9ºC at 06:00, rising to 53.2ºC and 41.0ºC at 15:00.

Correlating scenarios with receptors revealed discernible variations in thermal stress conditions, indicating specific environmental influences. Optimal thermal comfort levels were observed during the initial and final hours of the day, with adaptive measures necessary during hotter afternoon hours. Despite being estimated, thermal comfort indices play a pivotal role in decision-making for outdoor activities, urban planning, and public health to enhance climatic comfort. It's crucial to acknowledge these indices as preliminary references, subject to variation based on individual perceptions and unaccounted factors. Understanding this data contributes to well-being and security across diverse contexts, guiding practical decisions and climate adaptation strategies.

The implications of this study emphasize the importance of considering urban morphology and the interaction between built elements and open spaces in the analysis of the urban microclimate, as well as the understanding of interactions between urban configuration, solar exposure, and thermal comfort in different urban sectors. The study suggests that verticalization and urban density have a direct effect on thermal modes, ventilation, and human comfort. The analysis of correlations between vegetation, the Sky View Factor (SVF), Mean Radiant Temperature (MRT), and other climatic variables provides insights into how the built environment can impact urban thermal well-being. The results highlight the need to

apply more sustainable strategies in urban planning, such as increasing soil permeability and incorporating vegetation, to mitigate the effects of urban heat islands. These findings further strengthen the literature on architecture and urbanism, promoting more sustainable practices adapted to the effects of climate change.

Despite the depth of the analysis, several limitations should be considered. The study focused on specific urban sectors, which may not reflect the complexities of other cities with different climatic and geographical configurations. It is noted that the defined methodology does not account for factors such as human behavior and building use, which affect thermal variations and thermal comfort. Additionally, this study did not address the long-term dynamics of climate change, which could influence other conclusions. Future evaluations may incorporate these factors by expanding the analysis to different urban and climatic contexts. Although the calibrated model demonstrated strong correlations and error values within acceptable limits, the limitations include reliance on meteorological data from a single station and the need for adjustments in simulation parameters to better represent local characteristics. The diversity of urban sectors and the versatility of building materials could have been more thoroughly explored, suggesting that future research should expand to include various urban typologies and materials.

The discussion of the results highlights that integrated urban planning actions—involving the incorporation of vegetation, urban form regulation, careful selection of surface materials, and control of building density—can modify the microclimate and significantly improve thermal comfort in public spaces. Such measures also help reduce the population's vulnerability to heat extremes, reinforcing sustainable urban planning policies. Several studies support these findings, including those by Feng et al. (2024), Yilmaz et al. (2021), and Krüger (2017), which demonstrate that simulation methodologies and microclimatic analysis combined with innovative approaches, the use of high-reflectance materials, and the adoption of specific plant species constitute effective strategies for mitigating heat islands and ensuring urban thermal comfort. These findings have direct implications ranging from neighborhood design to normative decisions about density indices and municipal urban planning guidelines.

The findings align with studies such as Feng et al. (2024), which demonstrate vegetation's capacity to reduce mean radiant temperature (MRT) by up to 5 °C in comparable Asian contexts, and Habibi and Kahe (2024), which underscore the efficacy of green infrastructure in enhancing ventilation within densely built environments. In João Pessoa, verticalization-induced reductions in sky view factor (SVF) exacerbate thermal discomfort (PET 34–53 °C at 15:00), yet vegetation mitigates these effects, consistent with de Souza e Silva et al. (2022).

Regarding practical applications, it is observed that the strategies discussed have high replication potential in cities located in tropical and subtropical regions. International literature underlines that new predictive models and precise thermal comfort parameterizations enable anticipating critical scenarios and proposing solutions based on scientific knowledge and technological innovation. Such approaches are applicable across multiple scales—from lots or blocks to neighborhood configurations—and guide balanced verticalization practices, while also promoting the strengthening of green infrastructure. Observed experiences worldwide show that public and private interventions based on these principles contribute to more resilient and inclusive urban settlements. Thus, this is an interdisciplinary field

where urbanism, climatology, landscaping, and public health converge to build cities better adapted to the challenges posed by environmental changes.

Finally, it is recommended to enhance the literature review and discussion by incorporating recent studies on urban microclimates and innovative methodological investigations conducted in different geographic contexts. The works of Feng et al. (2024) and Yilmaz et al. (2021), as suggested by the reviewer, illustrate global trends in climate model calibration, adaptive public space design, and the use of new technologies for thermal mitigation. The critical reference and analysis of these contributions add academic rigor to the manuscript and position the study at the forefront of international scientific knowledge. Moreover, the discussion can be further improved by comparing obtained results with international examples, highlighting advances, limitations, and global trends related to the topic, especially those linked to advanced simulation models, mitigation strategies, and innovative materials.

Based on the findings of this study, to enhance urban planning and thermal comfort, it is recommended to develop public policies that implement the use of sustainable technologies and nature-based solutions. The increase in green infrastructure and strategies, shaded areas, and the use of construction materials with thermal properties suited to the local climate are essential to reduce urban temperatures and improve urban quality. Policies that promote verticalization with better density and increased soil permeability contribute to better air circulation and, in turn, favor a milder urban climate. Paying attention to the local microclimate when creating guidelines and policies for urban development can significantly influence thermal comfort and sustainability.

Although the results provided insights into thermal variations, the accuracy of the results obtained could be further analyzed by applying a more robust testing method. Future research could involve additional simulations with different calibration parameters to validate the results with greater precision. A sensitivity analysis could also be performed to assess the impact of external variables, such as changes in climatic conditions and adjustments in urban configuration.

5 Conclusions

In summary, understanding urban morphology and its interaction with elements such as lots, streets, and open spaces is fundamental for analyzing the urban microclimate. The impact of verticalization was assessed through computer simulation, aiding in predicting the effects of urban changes and supporting planning and sustainability policies. However, local characteristics, such as urban voids, mitigate this effect at certain points.

This study presents relevant contributions on the influence of urban morphology, particularly verticalization and vegetation factors, on microclimate and thermal comfort in João Pessoa. However, some limitations inherent to the adopted approach are noted. The main limitations include the limited spatial scope, as experiments and simulations focused on specific sectors, restricting the generalization of the results; the absence of detailed analysis on human behavior variability and dynamic building use; the reliance on a single meteorological station for validation, which may not capture all nuances of the local urban microclimate; and the lack of an analysis on long-term variations or trends associated with climate change.

The findings reveal that verticalization in low-latitude tropical cities with hot-humid climates reduces SVF and elevates temperatures (up to 30.5 °C in high-density scenarios), yet can be mitigated through vegetation and wind corridors, enhancing thermal comfort (PET and UTCI reductions of 2–4 °C). This necessitates revisions to urban planning regulations to limit building heights in low-ventilation areas while prioritizing 30% vegetative cover per lot.

Despite these limitations, the findings of this work converge with recent studies in literature. For instance, de Souza e Silva et al. (2022) observed that, in Brazilian tropical cities, the presence of vegetation and urban structure are closely related to thermal comfort and play a decisive role in mitigating heat islands, confirming trends identified in this study. Similarly, Dissanayake and Weerasinghe (2021) emphasized the relevance of adaptive strategies for urban microclimates in hot and humid cities, focusing on green areas and morphological planning. Akhavan et al. (2025) highlighted how innovative solutions in the urban environment can enhance outdoor thermal comfort. Therefore, compared to these works, this study helps broaden the understanding of the role of planned interventions in the built environment as a fundamental tool for promoting more resilient and comfortable cities for urban populations.

The results reported the significant effect of urban geometry, shading, and the thermal properties of construction materials on variations in relative humidity, Mean Radiant Temperature (MRT), and air velocity. It was found that the correlation between the Sky View Factor (SVF) and MRT revealed that areas with lower SVF exhibited higher temperatures due to greater heat retention and lower thermal diffusion, intensified by reduced ventilation in verticalized areas. Negative correlations between SVF and air velocity were observed in denser areas, contributing to heat stagnation and increased relative humidity.

Isolated verticalization elevates ambient temperatures and impairs ventilation; however, its integration with nature-based solutions (NBS) demonstrably enhances thermal comfort, as validated by an RMSE of 0.81 °C for the simulations.

Air humidity varied throughout the day, showing weak correlations with the Sky View Factor (SVF), while wind speed exhibited heterogeneity across sectors, significantly correlating with SVF. The relationship between SVF and humidity showed moderate to strong correlations ($-0.50 < r < 0.79$), indicating that a lower sky view leads to higher humidity due to reduced evaporation. This effect was most pronounced between 00:00 and 03:00, when shaded areas displayed increased humidity. Additionally, urban design and the arrangement of open spaces played an essential role in thermal regulation, as they define the amount of shading and ventilation permeability.

MRT variations displayed seasonal behavior, with maximum values exceeding 54.98 °C between 14:00 and 17:00, related to low relative humidity, high temperatures, and low air velocities. The effect of construction materials was evident in the thermal behavior of surfaces, as high thermal mass materials, such as concrete and asphalt, absorbed and retained heat throughout the day, resulting in higher nighttime temperatures and slower cooling. An efficient strategy for mitigating urban heat and improving thermal comfort includes materials with low thermal inertia and higher reflectance.

The analysis of Mean Radiant Temperature (MRT) revealed distinct correlation profiles across sectors, highlighting complex interactions between solar exposure, urban configuration, and material properties. Discrepancies with previous research emphasize the importance of a robust calibration approach, suggesting improvements in adjustment and

validation methods to ensure more reliable results in future studies. Thermal comfort indices demonstrated consistent patterns, indicating discomfort during the hottest hours, emphasizing the role of environmental and personal factors in thermal perception.

The model calibration process involved comparing measured data, simulated data, and values from the INMET station (A320), adjusting critical parameters to improve simulation accuracy. The procedure followed these steps: Data Collection and Pre-Processing. In situ measurements of air temperature and relative humidity were collected at different urban locations, considering variations in land use, verticalization, and vegetation cover. Data from the INMET station (A320) served as an external reference to verify deviations between the simulations and a less urbanized environment. Simulated data were obtained using the ENVI-met climate model, allowing comparison with real-world data.

To reduce the observed deviations between simulations and measured data, the parameters used in the model must be adjusted and improved based on previous studies and local urban characteristics, including atmospheric and radiation parameters. The roughness coefficient was adjusted to better represent the influence of urban roughness on airflow. The thermal conductivity of urban materials was refined based on local measurements and literature, considering high thermal inertia materials such as concrete and asphalt. The vegetation evapotranspiration coefficient was adjusted to enhance the simulation of cooling effects in green areas.

Ventilation and microclimate parameters were also considered, including initial wind speed, modified to better represent wind interaction with the urban environment, and soil moisture distribution, adjusted to improve the accuracy of relative humidity simulations.

To ensure the reliability of the results, calibration benchmarks from previous studies were used, including Root Mean Square Error (RMSE), comparing the average deviations between simulated and measured data, with values of 0.81 °C for air temperature and 2.13% for relative humidity, within the acceptable range observed in the literature (Feng et al., 2022; Habibi and Kahe, 2024; Sayad et al., 2024; Zheng et al., 2023). Pearson's Correlation Coefficient (R^2), where the model achieved $R^2 = 0.85$, indicating a strong correlation between simulated and measured values; and Spearman's Correlation Coefficient (r), applied to verify the relationship between the Sky View Factor (SVF) and temperature/humidity, revealing patterns consistent with previous studies.

For future research in this field, it is suggested to investigate the long-term impacts of climate change, considering IPCC RCP 8.5 scenarios combined with verticalization, across multiple Northeastern Brazilian cities, employing updated versions of ENVI-met with high-resolution data. Additionally, the role of innovative materials, such as supercool surfaces or permeable pavements alongside native vegetation in high-density scenarios, should be analyzed. Finally, studies on human behavior in public spaces under thermal discomfort (PET > 34 °C) are recommended as a priority, utilizing longitudinal surveys to validate locally adapted strategies in hot-humid climates.

Based on benchmarks, statistical tests, and the results obtained, further final adjustments should be made to minimize residual errors, as previously noted, ensuring greater accuracy for microclimatic analyses. The calibration process ensured that the simulations aligned with real-world data, providing an adequate representation of the impact of urban infrastructure on the urban microclimate. The adjusted parameters, along with the presented benchmarks, strengthen the reliability of the results for applications in urban planning and thermal comfort analysis. However, improvements, adjustments, and a review of the parameters used in the microclimatic model are still necessary.

These considerations are essential for advancing the understanding of the urban microclimate and ensuring projection accuracy in specific urban contexts. Thus, the results corroborate the importance of integrated strategies in urban planning to enhance ventilation, balance shading, and apply materials better suited to the local climate. Land use planning concerning buildings and open spaces should be designed to improve and promote thermal comfort and minimize urban heat islands due to climate change, such as selecting materials with lower heat retention capacity and implementing nature-based solutions, contributing to urban sustainability.

Funding The Article Processing Charge (APC) for the publication of this research was funded by the Coordenação de Aperfeiçoamento de Pessoal de Nível Superior - Brasil (CAPES) (ROR identifier: 00x0ma614). Capes-Coordenação de Aperfeiçoamento de Pessoal de Nível Superior.

Data availability The authors confirm that the data supporting the findings of this study are available in the article.

References

Aboelata, A., & Sodoudi, S. (2019). Evaluating urban vegetation scenarios to mitigate urban heat island and reduce buildings' energy in dense built-up areas in Cairo. *Building and Environment, 166*, Article 106407. https://doi.org/10.1016/j.buildenv.2019.106407

Acero, J. A., Koh, E. J. Y., Ruefenacht, L. A., & Norford, L. K. (2021). Modelling the influence of high-rise urban geometry on outdoor thermal comfort in Singapore. *Urban Climate, 36*, Article 100775. https://doi.org/10.1016/j.uclim.2021.100775

Akhavan, M., Alivirdi, M., Jamalpour, A., Kheradranjbar, M., Mafi, A., Jamalpour, R., & Ravanshadnia, M. (2025). Impact of Industry 5.0 on the construction industry (Construction 5.0): Systematic literature review and bibliometric analysis. *Buildings, 15*(9), Article 1491. https://doi.org/10.3390/buildings15091491

Altunkasa, C., & Uslu, C. (2020). Use of outdoor microclimate simulation maps for a planting design to improve thermal comfort. *Sustainable Cities and Society, 57*, Article 102137. https://doi.org/10.1016/j.scs.2020.102137

Andrade, P. C. R., & Romero, M. A. B. (2018). Análise do desempenho térmico dos materiais superficiais do contexto urbano do SIA/ DF. *Paranoá: Cadernos de Arquitetura e Urbanismo, 22*, 51–71. https://doi.org/10.18830/issn.1679-0944.n22.2018.04

Andrade, T. C., Nery, J., Miranda, S., Pitombo, C., Moura, T., & Katzschner, L. (2016). Medição do conforto térmico em áreas públicas urbanas de Salvador-BA e calibração do índice de conforto PET usando a técnica árvore de decisão. *Revista Eletrônica de Gestão e Tecnologias Ambientais, 4*(2), 278. https://doi.org/10.9771/gesta.v4i2.16821

Apreda, C., Reder, A., & Mercogliano, P. (2020). Urban morphology parameterization for assessing the effects of housing blocks layouts on air temperature in the Euro-Mediterranean context. *Energy and Buildings, 223*, Article 110171. https://doi.org/10.1016/j.enbuild.2020.110171

Apreda, C., Schulz, J., Reder, A., & Mercogliano, P. (2023). Survey of land cover datasets for updating the imperviousness field in urban parameterisation scheme TERRA_URB for climate and weather applications. *Urban Climate, 49*, Article 101535.

Aram, F., García, E., Solgi, E., & Mansournia, S. (2019). Urban green space cooling effect in cities. *Heliyon*. https://doi.org/10.1016/j.heliyon.2019.e01339

Ascione, F., Böttcher, O., Manniti, G., Mastellone, M., & Mühle, J. (2024). The effect of climate change and urbanization on outdoor microclimate: A case study in Berlin. *Energy and Buildings*. https://doi.org/10.1016/j.enbuild.2024.114024

Asfour, O. S., Mohsen, O., & Al-Qawasmi, J. (2023). Shading performance of public open spaces: A multi-criteria evaluation framework for housing projects. *Buildings*. https://doi.org/10.3390/buildings13123099

Bakhtyari, V., Fattahi, K., Movahed, K., & Franz, A. (2024). Investigating the effect of living walls on cooling energy consumption in various urban microclimates, building heights, and greenery coverage areas. *Sustainability (Switzerland)*. https://doi.org/10.3390/su16020920

Battisti, A. (2020). Bioclimatic architecture and urban morphology. Studies on intermediate urban open spaces. *Energies, 13*(21), Article 5819. https://doi.org/10.3390/en13215819

Battisti, A., Laureti, F., Zinzi, M., & Volpicelli, G. (2018). Climate mitigation and adaptation strategies for roofs and pavements: A case study at Sapienza University Campus. *Sustainability (Switzerland)*. https://doi.org/10.3390/su10103788

Bedra, K. B., Zheng, B., Li, J., & Luo, X. (2023). A parametric-simulation method to study the interconnections between urban-street-morphology indicators and their effects on pedestrian thermal comfort in tropical summer. *Sustainability*. https://doi.org/10.3390/su15118902

Binabid, J., & Anteet, Q. (2024). Numerical study of vegetation effects on thermal comfort for outdoor spaces at a public school in hot and arid climate. *Environmental Advances*. https://doi.org/10.1016/j.envadv.2023.100482

Blaine, B. (2023). I*ntroductory applied statistics: With resampling methods & R*. Springer Cham. https://doi.org/10.1007/978-3-031-27741-2

Blanco, I., & Convertino, F. (2023). Thermal performance of green façades: Research trends analysis using a science mapping approach. *Sustainability (Switzerland)*. https://doi.org/10.3390/su15139981

Boccalatte, A., Fossa, M., Thebault, M., Ramousse, J., & Ménézo, C. (2023). Mapping the urban heat island at the territory scale: An unsupervised learning approach for urban planning applied to the Canton of Geneva. *Sustainable Cities and Society, 96*, Article 104677. https://doi.org/10.1016/j.scs.2023.104677

Boeri, A., Longo, D., Fabbri, K., Roversi, R., & Boulanger, S. (2023). The relation between outdoor microclimate and people flow in historic city context the case study of Bologna within the ROCK project. *Sustainability (Switzerland)*. https://doi.org/10.3390/su15097527

Brahimi, M., Benabbas, M., & Djaghrouri, D. (2023). Setting up the ENVI-met digital tool to evaluate climatic conditions at an urban scale: A case study of Djelfa, Algeria. *Journal of the Bulgarian Geographical Society, 49*, 113–127. https://doi.org/10.3897/jbgs.e113695

Bruse, M., & Fleer, H. (1998). Simulating surface–plant–air interactions inside urban environments with a three dimensional numerical model. *Environmental Modelling & Software, 13*(3–4), 373–384. https://doi.org/10.1016/S1364-8152(98)00042-5

Chan, S. Y., & Chau, C. K. (2021). On the study of the effects of microclimate and park and surrounding building configuration on thermal comfort in urban parks. *Sustainable Cities and Society, 64*, Article 102512. https://doi.org/10.1016/j.scs.2020.102512

Chatzinikolaou, E., Chalkias, C., & Dimopoulou, E. (2018). Urban microclimate improvement using envi-met climate model. *The International Archives of the Photogrammetry, Remote Sensing and Spatial Information Sciences, XLII*(4), 69–76. https://doi.org/10.5194/isprs-archives-XLII-4-69-2018

da Silva, J. M. (2023). Influence of tree vegetation on thermal comfort in urban areas. *Revista Brasileira De Geografia Fisica, 16*(1), 633–645. https://doi.org/10.26848/rbgf.v16.1.p633-645

de Quadros, B. M., & Mizgier, M. G. O. (2023). Urban green infrastructures to improve pedestrian thermal comfort: A systematic review. *Urban Forestry and Urban Greening*. https://doi.org/10.1016/j.ufug.2023.128091

de Souza e Silva, R., da Silva, R. M., de Freitas, A. F., et al. (2022). Thermal comfort conditions at microclimate scale and surface urban heat island in a tropical city: A study on João Pessoa city, Brazil. *International Journal of Biometeorology, 66*, 1079–1093. https://doi.org/10.1007/s00484-022-02260-y

Dissanayake, C., & Weerasinghe, U. G. D. (2021). Urban microclimate and outdoor thermal comfort of public spaces in warm-humid cities: A comparative bibliometric mapping of the literature. *American Journal of Climate Change, 10*(4), 643–661. https://doi.org/10.4236/ajcc.2021.104023

Erlwein, S., & Pauleit, S. (2021). Trade-offs between urban green space and densification: Balancing outdoor thermal comfort, mobility, and housing demand. *Urban Planning, 6*(1), 5–19. https://doi.org/10.17645/UP.V6I1.3481

Fachinello Krebs, L., & Johansson, E. (2021). Influence of microclimate on the effect of green roofs in Southern Brazil – A study coupling outdoor and indoor thermal simulations. *Energy and Buildings, 241*, Article 110963. https://doi.org/10.1016/j.enbuild.2021.110963

Feng, L., Shuai, L., Zhou, Y., Zhang, X., & Sun, J. (2024). Improving the green space arrangement in residential areas from the perspective of tree leaf temperature utilizing scenario simulation in ENVI-met. *Science of the Total Environment*. https://doi.org/10.1016/j.scitotenv.2024.170650

Feng, Y., Wang, J., Zhou, W., Li, X., & Yu, X. (2022). Evaluating the cooling performance of green roofs under extreme heat conditions. *Frontiers in Environmental Science, 10*, Article 874614. https://doi.org/10.3389/fenvs.2022.874614

Fernandes, M. E., & Masiero, É. (2020). Relationship between outdoor thermal comfort and Local Climate Zones. *Urbe. Revista Brasileira de Gestão Urbana, 12*, e20190247. https://doi.org/10.1590/2175-3369.012.e20190247

Ferrarezi, H. S., Sousa, M. N. P. O., & Monteiro, E. Z. (2023). Estratégias de mitigação de calor em climas tropicais. *Vernácula - Territórios Contemporâneos, 1*(1). https://doi.org/10.18312/verncula.v1i1.2306

Fiorillo, E., Brilli, L., Carotenuto, F., Cremonini, L., Gioli, B., Giordano, T., & Nardino, M. (2023). Diurnal outdoor thermal comfort mapping through ENVI-met simulations, remotely sensed and in situ measurements. *Atmosphere, 14*(4), 641. https://doi.org/10.3390/atmos14040641

Gamero-Salinas, J., Kishnani, N., Sánchez-Ostiz, A., Monge-Barrio, A., & Benitez, E. (2022). Porosity, openness, and exposure: Identification of underlying factors associated with semi outdoor spaces' thermal performance and clustering in tropical high-density Singapore. *Energy and Buildings, 272*, Article 112339. https://doi.org/10.1016/j.enbuild.2022.112339

Ge, J., Wang, Y., Zhou, D., Gu, Z., & Meng, X. (2024). Effects of urban vegetation on microclimate and building energy demand in winter: An evaluation using coupled simulations. *Sustainable Cities and Society, 102*, Article 105199. https://doi.org/10.1016/j.scs.2024.105199

Gusson, C. D. S. (2020). O impacto da verticalização no microclima urbano e no conforto térmico na escala do pedestre: O papel da geometria e da envoltória dos edifícios [Doutorado em Tecnologia da Arquitetura, Universidade de São Paulo]. https://doi.org/10.11606/T.16.2020.tde-29032021-104403

Gusson, C. S., & Duarte, D. H. S. (2016). Effects of built density and urban morphology on urban microclimate—Calibration of the model ENVI-met V4 for the subtropical Sao Paulo, Brazil. *Procedia Engineering, 169*, 2–10. https://doi.org/10.1016/j.proeng.2016.10.001

Habibi, A., & Kahe, N. (2024). Evaluating the role of green infrastructure in microclimate and building energy efficiency. *Buildings, 14*(3), Article 825. https://doi.org/10.3390/buildings14030825

Hashemi, F., Poerschke, U., Iulo, L. D., & Chi, G. (2023). Urban microclimate, outdoor thermal comfort, and socio-economic mapping: A case study of Philadelphia, PA. *Buildings, 13*(4), Article 1040. https://doi.org/10.3390/buildings13041040

Instituto Brasileiro de Geografia e Estatística [IBGE]. (2023). *Censo Demográfico 2022: Primeiros resultados de população e domicílios*. https://censo2022.ibge.gov.br/

Instituto Nacional de Meteorologia [INMET]. (2022). *Normais climatológicas do Brasil 1991- 2020* [Arquivo PDF]. Ministério da Agricultura e Pecuária. https://portal.inmet.gov.br/normais

Jamei, E., Thirunavukkarasu, G., Chau, H., Seyedmahmoudian, M., Stojcevski, A., & Mekhilef, S. (2023). Investigating the cooling effect of a green roof in Melbourne. *Building and Environment*. https://doi.org/10.1016/j.buildenv.2023.110965

Kotharkar, R., & Dongarsane, P. (2024). Investigating outdoor thermal comfort variations across Local Climate Zones in Nagpur, India, using ENVI-met. *Building and Environment*. https://doi.org/10.1016/j.buildenv.2023.111122

Kowe, P., Mutanga, O., Odindi, J., & Dube, T. (2024). Impacts of eco-environmental quality, spatial configuration, and landscape connectivity of urban vegetation patterns on seasonal land surface temperature in Harare metropolitan city, Zimbabwe. *African Geographical Review, 43*(1), 125–143. https://doi.org/10.1080/19376812.2022.2117215

Krüger, E., Rossi, F., & Drach, P. (2017). Calibration of the physiological equivalent temperature index for three different climatic regions. *International Journal of Biometeorology, 61*(7), 1323–1336. https://doi.org/10.1007/s00484-017-1310-8

Lai, D., Lian, Z., Liu, W., Guo, C., Liu, W., Liu, K., & Chen, Q. (2020). A comprehensive review of thermal comfort studies in urban open spaces. *Science of the Total Environment*. https://doi.org/10.1016/j.scitotenv.2020.140092

Lai, D., Liu, W., Gan, T., Liu, K., & Chen, Q. (2019). A review of mitigating strategies to improve the thermal environment and thermal comfort in urban outdoor spaces. *Science of the Total Environment, 661*, 337–353. https://doi.org/10.1016/j.scitotenv.2019.01.062

Leal, L. P. S., & Barbosa, R. V. R. (2022). Conforto térmico em cânions urbanos verticalizados de cidade litorânea em clima tropical quente e úmido. In *Anais do XIX Encontro Nacional de Tecnologia do Ambiente Construído, 19*, 1–11. https://doi.org/10.1007/s00484-0061-8

Li, J., Mao, Y., Ouyang, J., & Zheng, S. (2022). A review of urban microclimate research based on CiteSpace and VOSviewer analysis. *International Journal of Environmental Research and Public Health*. https://doi.org/10.3390/ijerph19084741

Lin, L., & Gui, Y. (2024). Why does the courtyard spaces of same ethnic group present diverse characteristics in different regions: Evidence based on ENVI-met climate modeling. *Journal of Cleaner Production, 466*, Article 142703. https://doi.org/10.1016/j.jclepro.2024.142703

Liu, Z., Cheng, K. Y., Sinsel, T., Simon, H., Jim, C. Y., Morakinyo, T. E., He, Y., Yin, S., Ouyang, W., Shi, Y., & Ng, E. (2023). Modeling microclimatic effects of trees and green roofs/façades in ENVI-met: Sensitivity tests and proposed model library. *Building and Environment*. https://doi.org/10.1016/j.buildenv.2023.110759

Li, X., Yang, B., Liang, F., Zhang, H., Xu, Y., & Dong, Z. (2023). Modeling urban canopy air temperature at city-block scale based on urban 3D morphology parameters- A study in Tianjin, North China. *Building and Environment*. https://doi.org/10.1016/j.buildenv.2023.110000

Matzarakis, A., Rutz, F., & Mayer, H. (2007). Modelling radiation fluxes in simple and complex environments—application of the RayMan model. *International Journal of Biometeorology, 51*(4), 323–334. https://doi.org/10.1007/s00484-006-0061-8

Matzarakis, A., Rutz, F., & Mayer, H. (2010). Modelling radiation fluxes in simple and complex environments: Basics of the RayMan model. *International Journal of Biometeorology, 54*(2), 131–139. https://doi.org/10.1007/s00484-009-0261-0

McRae, I., Freedman, F., Rivera, A., Li, X., Dou, J., Cruz, I., Ren, C., Dronova, I., Fraker, H., & Bornstein, R. (2020a). Integration of the WUDAPT, WRF, and ENVI-met models to simulate extreme daytime temperature mitigation strategies in San Jose, California. *Building and Environment*. https://doi.org/10.1016/j.buildenv.2020.107180

McRae, I., Freedman, F., Rivera, A., Li, X., Dou, J., Cruz, I., Ren, C., Dronova, I., Fraker, H., & Bornstein, R. (2020b). Integration of the WUDAPT, WRF, and ENVI-met models to simulate extreme daytime temperature mitigation strategies in San Jose, California. *Building and Environment, 184*, Article 107180. https://doi.org/10.1016/j.buildenv.2020.107180

Medeiros, M. O., Patriota, E. G., & Coelho, H. R. (2023). A relação entre ilhas de calor urbana superficial, ocupação do solo e conforto térmico: Um estudo da cidade de João Pessoa, Brasil. *Encontro nacional de conforto no ambiente construído, 17*, 1–10. https://doi.org/10.46421/encac.v17i1.3756

Noda, L., Leder, S. M., & Lima, A. V. P. (2022). Trabalhar em casa é mais confortável? Avaliação do conforto térmico de ocupantes em trabalho remoto. *Encontro nacional de tecnologia do ambiente construído, 19*, 1–13.

Normais *Climatológicas do Brasil 1991–2010, Instituto Nacional de Meteorologia (INMET)*. (n.d.). Retrieved January 7, 2024, from https://portal.inmet.gov.br/uploads/normais/NORMAISCLIMATOLOGICAS.pdf

Norouziasas, A., Pilehchi Ha, P., Ahmadi, M., & Rijal, H. B. (2022). Evaluation of urban form influence on pedestrians' wind comfort. *Building and Environment, 224*, Article 109522. https://doi.org/10.1016/j.buildenv.2022.109522

Oke, T. R., Mills, G., Christen, A., & Voogt, J. A. (2017). *Urban Climates* (1st ed.). Cambridge University Press. https://doi.org/10.1017/9781139016476

Piercy, C., Charbonneau, B., Russ, E., & Swannack, T. (2024). Examining the commonalities and knowledge gaps in coastal zone vegetation simulation models. *Earth Surface Processes and Landforms, 49*(1), 24–48. https://doi.org/10.1002/esp.5565

Ramyar, R., Ramyar, A., Kialashaki, Y., Bryant, M., & Ramyar, H. (2019). Exploring reconfiguration scenarios of high-density urban neighborhoods on urban temperature–the case of Tehran (Iran). *Urban Forestry & Urban Greening, 44*, Article 126398. https://doi.org/10.1016/j.ufug.2019.126398

Ribeiro, I., Martilli, A., Falls, M., Zonato, A., & Villalba, G. (2021). Highly resolved WRF-BEP/BEM simulations over Barcelona urban area with LCZ. *Atmospheric Research, 248*, Article 105220. https://doi.org/10.1016/j.atmosres.2020.105220

Roshan, G., Almomenin, H., Hirashima, S., & Attia, S. (2019). Estimate of outdoor thermal comfort zones for different climatic regions of Iran. *Urban Climate, 27*, 8–23. https://doi.org/10.1016/j.uclim.2018.10.005

Santamouris, M., Ban-Weiss, G., Osmond, P., Paolini, R., Synnefa, A., Cartalis, C., Muscio, A., Zinzi, M., Morakinyo, T. E., Ng, E., Tan, Z., Takebayashi, H., Sailor, D., Crank, P., Taha, H., Pisello, A. L., Rossi, F., Zhang, J., & Kolokotsa, D. (2018). Progress in urban greenery mitigation science – Assessment methodologies advanced technologies and impact on cities. *Journal of Civil Engineering and Management, 24*(8), 638–671. https://doi.org/10.3846/jcem.2018.6604

Santana, T. C., Guiselini, C., Montenegro, A. A. A., Pandorfi, H., da Silva, R. A. B., da Silva e Silva, R., Batista, P. H. D., Cavalcanti, S. D. L., Gomes, N. F., da Silva, M. V., & Jardim, A. M. R. F. (2023). Green roofs are effective in cooling and mitigating urban heat islands to improve human thermal comfort. *Modeling Earth Systems and Environment, 9*(4), 3985–3998. https://doi.org/10.1007/s40808-023-01743-0

Sayad, B., Helmi, M., Osra, O., Abed, A., Alhubashi, H., Renard, F., & Alonso, L. (2024). Microscale investigation of Urban Heat Island (UHI) in Annaba City: Unveiling factors and mitigation strategies. *Sustainability*. https://doi.org/10.3390/su16020747

Shinzato, P., Simon, H., Silva Duarte, D. H., & Bruse, M. (2019). Calibration process and parametrization of tropical plants using ENVI-met V4 – Sao Paulo case study. *Architectural Science Review, 62*(2), 112–125. https://doi.org/10.1080/00038628.2018.1563522

Silva Neto, J. A., & Sales, M. C. L. (2020). [Título do artigo não especificado]. *Revista Brasileira de Climatologia, 26*, 833–853. https://doi.org/10.5380/abclima.v26i0

Sinsel, T., Simon, H., Broadbent, A., Bruse, M., & Heusinger, J. (2021). Modeling the outdoor cooling impact of highly radiative "super cool" materials applied on roofs. *Urban Climate*. https://doi.org/10.1016/j.uclim.2021.100898

Sinsel, T., Simon, H., Ouyang, W., Dos Santos Gusson, C., Shinzato, P., & Bruse, M. (2022). Implementation and evaluation of mean radiant temperature schemes in the microclimate model ENVI-met. *Urban Climate, 45*, Article 101279. https://doi.org/10.1016/j.uclim.2022.101279

Souza, J. F. D., Silva, R. M., & Silva, A. M. (2016). Influência do uso e ocupação do solo na temperatura da superfície: O estudo de caso de João Pessoa - PB. *Ambiente Construído, 16*(1), 21–37. https://doi.org/10.1590/s1678-86212016000100058

Souza, V., & Katzschner, L. (2018). Mapa climático como ferramenta de gestão urbana: Estudo na cidade de João Pessoa/PB. In *Anais do 17º Encontro Nacional de Tecnologia do Ambiente Construído* (pp. 3900–3907). ANTAC. https://doi.org/10.46421/entac.v17i1.1837

Stark da Silva, P. W., Duarte, D., & Pauleit, S. (2023). The role of the design of public squares and vegetation composition on human thermal comfort in different seasons a quantitative assessment. *Land*. https://doi.org/10.3390/land12020427

Susca, T., Zanghirella, F., & Del Fatto, V. (2023). Building integrated vegetation effect on micro-climate conditions for urban heat island adaptation. Lesson learned from Turin and Rome case studies. *Energy and Buildings*. https://doi.org/10.1016/j.enbuild.2023.113233

Wai, C. Y., Tariq, M. A. U. R., & Muttil, N. (2022). A systematic review on the existing research, practices, and prospects regarding urban green infrastructure for thermal comfort in a high-density urban context. *Water*. https://doi.org/10.3390/w14162496

Wu, T., Cao, B., & Zhu, Y. (2018). A field study on thermal comfort and air-conditioning energy use in an office building in Guangzhou. *Energy and Buildings, 168*, 428–437. https://doi.org/10.1016/j.enbuild.2018.03.030

Wu, Z., Dou, P., & Chen, L. (2019). Comparative and combinative cooling effects of different spatial arrangements of buildings and trees on microclimate. *Sustainable Cities and Society, 51*, Article 101711. https://doi.org/10.1016/j.scs.2019.101711

Xie, J., Li, X., Chung, L., & Webster, C. (2024). Effects of land surface temperatures on vegetation phenology along urban-rural local climate zone gradients. *Landscape Ecology, 39*(3), 62. https://doi.org/10.1007/s10980-024-01856-6

Yang, L., Zhang, L., Stettler, M., Sukitpaneenit, M., Xiao, D., & van Dam, K. (2020). Supporting an integrated transportation infrastructure and public space design: A coupled simulation method for evaluating traffic pollution and microclimate. *Sustainable Cities and Society*. https://doi.org/10.1016/j.scs.2019.101796

Yi, C., Kwon, H., & Yang, H. (2022). Spatial temperature differences in local climate zones of Seoul metropolitan area during a heatwave. *Urban Climate, 41*, 101012. https://doi.org/10.1016/j.uclim.2021.101012

Yilmaz, B., Asokkumar, A., Jasiuniene, E., & Kazys, R. (2020). Air-Coupled, Contact, and Immersion Ultrasonic Non-Destructive Testing: Comparison for Bonding Quality Evaluation. *Applied Sciences-Basel, 10*(19), 6757. https://doi.org/10.3390/app10196757

Yilmaz, S., Mutlu, B. E., Aksu, A., Mutlu, E., & Qaid, A. (2021). Street design scenarios using vegetation for sustainable thermal comfort in Erzurum, Turkey. *Environmental Science and Pollution Research, 28*(3), 3672–3693. https://doi.org/10.1007/s11356-020-10555-z

Yi, P., Liu, L., Huang, Y., Zhang, M., Liu, H., & Bedra, K. B. (2023). Study on the coupling relationship between thermal comfort and urban center spatial morphology in summer. *Sustainability, 15*(6), Article 5084. https://doi.org/10.3390/su15065084

Zhang, P., Ghosh, D., & Park, S. (2023). Spatial measures and methods in sustainable urban morphology: A systematic review. *Landscape and Urban Planning, 237*, Article 104776. https://doi.org/10.1016/j.landurbplan.2023.104776

Zhang, W., Huo, H., Geng, X., Zhou, P., Guo, L., & Li, Z. (2023). Simulation of canopy urban heat island at a block scale based on local climate zones and urban weather generator: A case study of Beijing. *International Journal of Remote Sensing*. https://doi.org/10.1080/01431161.2023.2203344

Zhao, J., Chen, G., Yu, L., Ren, C., Xie, J., Chung, L., Ni, H., & Gong, P. (2023). Mapping urban morphology changes in the last two decades based on local climate zone scheme: A case study of three major urban agglomerations in China. *Urban Climate*. https://doi.org/10.1016/j.uclim.2022.101391

Zheng, X., Kong, F., Yin, H., Middel, A., Yang, S., Liu, H., & Huang, J. (2023). Green roof cooling and carbon mitigation benefits in a subtropical city. *Urban Forestry & Urban Greening, 86*, Article 128018. https://doi.org/10.1016/j.ufug.2023.128018